Ortiz Alejandra (Orcid ID: 0000-0003-3780-0952)

ZHANG Yingqi (Orcid ID: 0000-0001-7783-8336)

# A distinguishing feature of *Pongo* upper molars and its implications for the taxonomic identification of isolated hominid teeth from the Pleistocene of Asia

Alejandra Ortiz[1,2], Shara E. Bailey[1,3], Miguel Delgado[4,5], Clément Zanolli[6], Fabrice Demeter[7], Anne-Marie Bacon[8], Thi Mai Huong Nguyen[9], Anh Tuan Nguyen[9], Yingqi Zhang[10], Terry Harrison[1], Jean-Jacques Hublin[3], Matthew M. Skinner[3,12]

[1] Department of Anthropology, New York University, New York, NY, USA

[2] Institute of Human Origins, Arizona State University, Tempe, AZ, USA

[3] Department of Human Evolution, Max Planck Institute for Evolutionary Anthropology, Leipzig, Germany

[4] División Antropología, Facultad de Ciencias Naturales y Museo, Universidad Nacional de La Plata, La Plata, República Argentina

[5] Consejo Nacional de Investigaciones Científicas y Técnicas CONICET, República Argentina

[6] Laboratoire AMIS, UMR 5288 CNRS, Université de Toulouse, France

[7] Département Homme Nature Société, Unité Mixte de Recherche 7206, Unité Scientifique du Muséum 104, Muséum National d'Histoire Naturelle, Musée de l'Homme, Paris, France



This is the author manuscript accepted for publication and has undergone full peer review but has not been through the copyediting, typesetting, pagination and proofreading process, which may lead to differences between this version and the Version of Record. Please cite this article as doi: 10.1002/ajpa.23928

[8] Laboratoire BABEL, FRE 2029 CNRS, Université Paris Descartes, Faculté de chirurgie dentaire, Montrouge, France

[9] Anthropological and Palaeoenvironmental Department, The Institute of Archaeology, Hanoi, Vietnam

[10] Key Laboratory of Vertebrate Evolution and Human Origins, Institute of Vertebrate Paleontology and Paleoanthropology (IVPP), Chinese Academy of Sciences, Beijing, People's Republic of China

[11] State Key Laboratory of Palaeobiology and Stratigraphy, Nanjing Institute of Geology and Palaeontology, Chinese Academy of Sciences, Nanjing 210008, China

[12] School of Anthropology and Conservation, University of Kent, Canterbury, United Kingdom

* Corresponding author.

E-mail address: ao706@nyu.edu (A. Ortiz)

**Abstract**

**Objectives**

The taxonomic status of isolated hominoid teeth from the Asian Pleistocene has long been controversial due to difficulties distinguishing between pongine and hominin molars given their high degree of morphometrical variation and overlap. Here we combine non-metric and geometric morphometric data to document a dental pattern that appears to be taxonomically diagnostic among *Pongo*. We focus on the protoconule, a cuspule of well-documented evolutionary history, as well as on shape differences of the mesial fovea of the upper molars.

**Materials and Methods**

We examined 469 upper molars of eight hominid genera (*Australopithecus*, *Paranthropus*, *Homo*, *Meganthropus*, *Sivapithecus*, *Pan*, *Gorilla*, and *Pongo*), including representatives of

*Homo erectus* and extinct and recent *Pongo*. Analyses were conducted at the enamel-dentine junction to overcome the limitations introduced by dental wear.

**Results**

We found that a moderate or large protoconule is present in ~80% of Pleistocene and extant *Pongo*. Conversely, a moderate to pronounced protoconule in hominins, *Meganthropus*, and African great apes occurs in low frequencies (~0%-20%). Canonical variate analyses for the mesial fovea show that Pleistocene and extant *Pongo* cluster together and are clearly differentiated from all other groups, except for *Sivapithecus*.

**Discussion**

This study suggests that the protoconule and the shape of the mesial fovea in upper molars are useful features for the taxonomic identification of isolated hominid teeth. By identifying these new features, our results can contribute to the better understanding of hominoid evolutionary history and biogeography during the Asian Pleistocene. However, we emphasize that the reported features should be used in combination with other diagnostic variables for the most accurate taxonomic assessments.

**Key words:** Protoconule; mesial fovea; enamel-dentine junction; taxonomy; hominids

## 1. Introduction

Hominid biogeography in Asia during the Pleistocene is characterized by a complex scenario where at least four genera – *Pongo*, *Homo*, *Gigantopithecus*, and *Meganthropus* ( – coexisted in mainland and island Asia (Ciochon, 2009; Zanolli et al., 2019). Although orangutans are today restricted to Borneo (*Pongo pygmaeus*) and northern Sumatra (*Pongo abelii* and *Pongo tapanuliensis*) (Nater et al., 2017), they were widely distributed in China, Vietnam, Thailand, Laos, Cambodia, Peninsular Malaysia, Borneo, Sumatra, and Java during the

Pleistocene (Bacon & Long, 2001, 2002; Bacon et al., 2008; Ciochon, Olsen, & James, 1990; Groves, 2001; Harrison, 1998, 2000; Harrison, Krigbaum, & Manser, 2006; Harrison, Jin, Zhang, & Wang, 2014; Hooijer, 1948; Ibrahim et al., 2013; Kaifu, Fachroel, & Baba, 2001; Nisbett and Ciochon, 1993; Olsen & Ciochon, 1990; Schwartz, Long, Cuong, Kha, & Tattersall, 1994, 1995; Spehar et al., 2018; Wang et al., 2014; Zhao, Wang, Jin, Qin, & Pan, 2009). The oldest known *Pongo* fossils date to the Early Pleistocene of southern China, and members of this genus possibly survived until the early Holocene in Vietnam and Cambodia (Drawhorn, 1995; Harrison et al., 2006; Schwartz et al., 1994, 1995). The earliest occurrence of orangutans in the islands of Southeast Asia has proven more difficult to ascertain. Several dental remains from Sangiran Dome and Trinil in Java, dated to the Early or Middle Pleistocene, have been attributed to *Homo erectus, Meganthropus paleojavanicus,* or *Pongo* sp.(Antón, 2003; de Vos, 2004; Harrison et al., 2006, 2014; Hooijer, 1948; Smith et al., 2009; Tyler, 2004; von Koenigswald, 1982; Zanolli, Grine, Kullmer, Schrenk, & Macchiarelli, 2015; Zanolli et al., 2019), with a few authors even suggesting morphological affinities with *Homo habilis*, *Paranthropus robustus*, *Australopithecus africanus* and *Pan* sp. (e.g., Tyler, 1991, 1995). In particular, the taxonomic affinities of the following specimens from Southeast Asia have been the subject of intense debate among scholars: Trinil 11620 and Trinil 11621 from Trinil, Indonesia, and SMF-8855, SMF-8864, SMF-8865, SMF-8879, SMF-8898, SMF-100055, S5, S6a, S7-9, S7-20, S7-53, S7-62, S7-64, S7-65, and S7-76 from Sangiran, Indonesia (reviewed in Smith et al., 2018; Zanolli et al., 2019).

The earliest definitive occurrence of *H. erectus* in Southeast Asia dates to ~1.6 Ma (Antón, 2003; Falguères et al., 2016; Larick et al., 2001; Swisher et al., 1994). Fossil evidence for the penecontemporaneous occurrence of *Homo* in China comes from Yuanmou (~1.7 Ma; Zhu et al., 2008), Gongwangling (~1.63 Ma; Zhu et al., 2015) and Shangshazui in the Nihewan Basin (~1.6-1.7 Ma; Ao, Dekkers, Wei, Qiang, & Xiao, 2013), and artefacts from the Paleolithic site of Shangchen suggest a hominin occupation of the Chinese Loess Plateau that dates to as early as ~2.1 Ma (Zhu et al., 2018). Dentognathic remains from Longgupo Cave in Chongqing Municipality (~1.4-1.8 Ma; Han et al., 2012), once thought to represent the earliest record of hominins in China, are now believed to belong to an extinct ape (Ciochon, 2009, 2010; Etler, Crummett, & Wolpoff, 2001; Schwartz and Tattersall, 1996). Although they have received less attention than Longgupo, several additional Pleistocene sites in China and Vietnam have yielded hominoid fossils of uncertain or contentious taxonomic status (see Ciochon, 2010) and these have been variously assigned to *Australopithecus*, *H. erectus*, *Homo* sp., cf. Ponginae, *Pongo* sp., *Hemanthropus, Langsonia* and Hominoidea (gen. et sp. indet.) (Ciochon, 2010; Harrison et al., 2014). In addition to specimens of known provenance discussed above, there are several isolated teeth from the von Koenigswald's Chinese Apothecary collection whose affinities have yielded varied opinions, but it appears that at least three hominoid groups are represented, including "*Hemanthropus peii*", *Sinanthropus officinal*is [= *Homo erectus*], and *Pongo* sp. (reviewed in Smith et al., 2018).

Many of the taxonomic uncertainties associated with Pleistocene hominoids in Asia stem from the problem of distinguishing between the molars of pongines and hominins, especially when they are worn, and this is compounded by the fact that many assemblages are composed of isolated teeth. Both pongines and hominins have relatively thick-enameled crenulated molars with a low occlusal topography (Fig. S1). Moreover, molars of these taxa overlap in crown formation times and daily secretion rates (Grine and Franzen, 1994; Martin, 1985; Olejniczak et al., 2008a; Smith, Olejniczak, Reid, Ferrell, & Hublin, 2006, Smith et al., 2011; Smith, 2016; but see Smith et al., 2018 for a recent comprehensive study on crown formation times in *Pongo* and *Homo*). It has also been suggested that the occlusal outline of *Pongo* upper molars is more oval than in African great apes and more similar in this regard to that of *Homo* (Swindler & Olshan, 1988). Several experts have noted the remarkable tooth size and shape variation observed in fossil *Pongo* (Harrison, 2000; Harrison et al., 2014; Schwartz et al., 1995). This observation is in line with the high degree of postcanine variation documented for extant *Pongo* in which there is no consistent dental morphological pattern within populations (Uchida, 1996, 1998; but see Pilbrow, 2018) and isolated teeth are difficult to separate at the species level (Harrison et al., 2014). Extinct and recent humans also exhibit a high degree of molar size variation, and both *Pongo* and *Homo* experienced similar overall trends of dental reduction over time (Demeter et al., 2004; Garn, Lewis, & Kerewsky, 1963; Goose, 1963; Grine & Franzen, 1994; Harrison et al., 2014; Hooijer, 1948; Schuman & Brace, 1954; Smith, 2016; Tshen, 2016; Weidenreich, 1937, 1945). This scenario becomes even more complex with the presence of a number of molars that,

while falling closer in size to early *Homo* than to *Pongo*, exhibit a more ape-like morphology (Ciochon, 2009, 2010).

The high frequency of supernumerary teeth in *Pongo* further complicates the taxonomic attribution of isolated hominid teeth from the Asian Pleistocene. Between 7% and 20% of *Pongo* individuals possess one or more supernumerary teeth, most of which (~85%) are upper and lower M4s (Bergstrom et al., 2016; Hooijer, 1948; Mahler, 1973; Selenka, 1898). When compared to their metameres, *Pongo* M4s are generally the smallest tooth in the molar row, with linear measurements falling well within the dimensions for *Homo*. While highly variable, M4s tend to retain the morphological features of their metameres and are not easily identified as supernumerary (Hooijer, 1948; Mahler, 1973). Thus, *Pongo* M4s could be easily confused with *Homo* molars, especially when only size variables are considered. This ambiguity has resulted in several isolated molar teeth from Pleistocene deposits being classified by different experts as either *Pongo* M4s or *Homo* sp./*Homo erectus* (Harrison et al., 2006; Schwartz et al., 1994, 1995; Smith et al., 2009).

Here we combine dental non-metric and geometric morphometric data to document a dental pattern on the upper molars that appears to be taxonomically diagnostic among Pleistocene and recent *Pongo*. We focused our analyses on the protoconule, a cuspule located on the mesial side of the protocone at the intersection of the preprotocrista and the hypoparacrista, as well as on shape differences of the mesial portion of the trigon between the protocone and paracone dentine horns. Specifically, we quantified patterns of intra and inter-group variation of

these features in a large sample of upper molars encompassing a wide range of fossil and extant hominid taxa and examined how well they differentiate isolated teeth of *Pongo* from those of *Homo* and other hominids. To overcome the limitations introduced by dental wear, which can obliterate informative features at the level of the outer enamel surface (OES), data collection and analyses were performed at the enamel-dentine junction (EDJ) (Olejniczak et al., 2008a; Ortiz, Bailey, Hublin, & Skinner, 2017; Skinner et al., 2008; Smith et al., 2018). The EDJ is the interface between the enamel cap and dentine crown and preserves the end point of growth of the inner enamel epithelium (Butler, 1956; Schour & Massler, 1940). Unless they are the result of dental tissue mineralization, which occurs later in morphogenesis, cusps (including small cuspules, conules, and tubercles) and crests develop as folds of the inner enamel epithelium (Butler, 1985). Thus, the study of the EDJ not only allows to more clearly determine topological relationships among dental structures (compared to the OES where these relationships may be masked by enamel deposition), but also represents an important means to distinguish between hominid taxa, even at the infraspecific level (e.g., Hanegraef et al., 2018; Macchiarelli et al., 2006; Machiarelli, Bondioli, & Mazurier, 2008; Macchiarelli, Bayle, Bondioli, Mazurier, & Zanolli, 2013;, 2008, 2013; Ortiz et al., 2017; Skinner et al., 2008, Skinner, Gunz, Wood, Boesch, & Hublin, 2009; Zanolli et al., 2014, 2015, 2018).

The protoconule (alternatively referred to as the paraconule) is part of the basic mammalian tribosphenic molar (Bown & Kraus, 1979; Butler, 1978, 1992; Crompton, 1971; Szalay, 1969; van Valen, 1966) with a long and well-documented evolutionary history. It is

generally present in early primates from the Paleocene and Eocene (Szalay & Delson, 1979), and is variably retained in extant strepsirrhines (Schwartz & Tattersall, 1985) and platyrrhines (Kay, 1980; Marivaux et al., 2016). A discernable protoconule is present in most stem catarrhines (i.e., propliopithecids, pliopithecoids, and dendropithecids) (Alba et al., 2010, Alba, Moyà-Solà, Robles, & Galindo, 2012; Cote, McNulty, Steven, & Nengo, 2016; Delson & Andrews, 1975; Harrison, 1982, 1988; Harrison & Gu, 1999; Harrison, Delson, & Jian, 1991; Harrison, van der Made, & Ribot, 2002; Rossie & MacLatchy, 2006; Szalay & Delson, 1979; Zhang & Harrison, 2008; although Godinot, 1994 contends that the protoconule is lacking in propliopithecids) and stem hominoids (i.e., proconsulids and afropithecids) (Andrews, 1978; Harrison, 1986, 2002, 2010; Harrison & Andrews, 2009; Le Gros Clark & Leakey, 1951; Pilbeam, 1969). A variably developed protoconule is also ubiquitous in fossil hominids from the Miocene of Africa and Eurasia (see Begun, 1992; Ishida & Pickford, 1997; Kordos & Begun, 1997; Kunimatsu et al, 2004; Pickford, 1985; Perez de los Rios, 2015; Pilbeam, Rose, Badgley, & Lipschutz, 1980; Suwa, Kono, Katoh, Asfaw, & Beyene, 2007; von Koenigswald, 1952; Zhang & Harrison, 2017). The presence of a protoconule can be inferred, therefore, to be a primitive primate feature that has been retained as part of the ancestral catarrhine and hominoid morphotypes (Delson & Andrews, 1975; Harrison, 1982, 1987). However, the frequency of occurrence and the degree of development of the protoconule among fossil catarrhines has not been documented.

Studies of the protoconule among extant hominoids date back to the late 1800s, with Selenka's (1898) comprehensive anatomical descriptions of *Pongo*. Selenka (1898) reported a

high incidence (76%-94% for females and 90%-100% for males, depending on serial position) of the protoconule in *Pongo* upper molars (see also Hooijer, 1948). Subsequent studies have documented the presence (in different frequencies and degrees of expression) of the protoconule in extant African apes (Korenhof, 1960; Pilbrow, 2003; Remane, 1960; Swindler, 1976; Swindler & Olshan, 1988). Pilbrow (2003) reported that 15-37% of *Pan paniscus* and 20-66% of *Pan troglodytes* upper molars have distinct protoconules. The cuspule has also been reported in humans, with an incidence ranging between ~5% and 45% depending on the population examined (Kanazawa et al., 1990). There are no published accounts of the occurrence of the protoconule in hylobatids, but anecdotal reports have indicated that the cuspule is either small in size or absent (Delson & Rosenberger, 1984; Szalay & Delson, 1979). A poorly expressed protoconule would be expected in hylobatids, given the characteristically low and rounded cusps and crests on the upper molars. A survey by TH of a sample (n=61) of *Hylobates* spp. found that a small but discernable protoconule was observable in 44% of M1s, 77% of M2s and 25% of M3s (unpublished data). The presence of a protoconule was also reported in a collection of fossil upper molars of *Nomascus* from the Pleistocene of southern China (Zhang et al., 2018). The lack of a more comprehensive comparative analysis of the protoconule using a large and diverse sample of hominoids has limited the implications of Selenka's (1898) initial observations on the high incidence of this cuspule in *Pongo* and its potential usefulness in hominoid systematics.

## 2. Materials and methods

*2.1. Sample*

Our study sample consists of 469 upper molars of eight hominid genera, including *Australopithecus*, *Paranthropus*, *Homo*, *Pan*, *Gorilla, Pongo, Sivapithecus*, and *Meganthropus*. Micro-computed tomography was used to image the EDJ of the upper molars (Table 1). All data were derived from original specimens and include the following taxa: *Australopithecus anamensis* (n=3), *Australopithecus afarensis* (n=7), *A. africanus* (n=39), *Paranthropus robustus* (n=41), *P. boisei* (n=4), early *Homo* (n=8), *H. erectus sensu lato* (n=7), Middle Pleistocene European hominins (MPEH, n=3), *Homo neanderthalensis* (n=57), *Homo sapiens* (n=95), *Pan troglodytes* (n=58), *Pan paniscus* (n=9), *Gorilla* sp. (n=28),*Pongo* sp. (n=105), *Sivapithecus* sp. (n=3), and *Meganthropus* sp. (n=2) . Samples with less than seven specimens were only analyzed at the generic level, except for *H. erectus s.l.* as this species is of primary interest for this study. The early *Homo* sample includes hominins classified as *Homo habilis*, *Homo rudolfensis*, and individuals from the Early Pleistocene whose affinities have been only identified as *Homo* sp. The *H. erectus s.l.* sample includes specimens from both Africa and Asia (KNM-ER 1808h M2, Sangiran 4 M1-3, Sangiran 7-3b M1, Sangiran 7-3c M2, and Sangiran 11 UM).The *Pongo* sample comprises specimens from the Pleistocene of China (n=25) and Vietnam (n=50), as well as extant *Pongo* (*P. abelii*=12, *P. pygmaeus*=8, and *Pongo* sp.=10). Furthermore, it should be noted that our *Meganthropus* sample is represented by Trinil 11620 and Trinil 11621, specimens with controversial affinities and that have been previously attributed to other taxa (see above, and Zanolli et al., 2019). Additional details of the fossil specimens used in this study are

provided in Table S1. We made no attempt to record the sex of the specimens given that our sample mainly comprises isolated teeth and that the sex is unknown for most fossils. However, previous studies have found that discrete traits do not significantly vary between sexes in great apes and hominins (Uchida, 1996; Pilbrow, 2003; Ortiz et al., 2017). Although some specimens in our sample exhibit moderate wear (up to Molnar's [1971] stage 5), this did not affect the accurate assessment of protoconule expression at the EDJ. However, specimens were not included in the geometric morphometric analysis if the tips of the protocone and/or paracone were worn or damaged.

The fossil *Pongo* material from China was recovered from Pleistocene cave deposits in Guangxi (Harrison et al., 2014) and was scanned with a TX225-Actis microCT system using the following parameters: 130 kV, 0.2-0.24 mA, and a 0.2 or 0.5 mm copper filter. The Pleistocene *Pongo* specimens from Vietnam come from Hang Hum, Lang Trang, Tham Khuyen and Tham Om Caves and were scanned with a v|tome|x L 240-180 instrument (90-100 kV, 400 µA, 0.1 mm copper) at the AST-RX platform of the MNHN Paris. The two Trinil molars (11620 and 11621) were scanned by synchrotron radiation-based µCT on beamline ID 19 of the European Synchrotron Radiation Facility at Grenoble using an absorption mode with an isotropic voxel size of 31.12 $\mu m^3$ at an energy of 60 keV10. The microCT datasets of these two specimens were downloaded from at the European Synchrotron Radiation Facility Paleontological Microtomographic Database (http://paleo.esrf.eu). The three *Sivapithecus* molars were scanned by X-ray computed microtomography at the Multidisciplinary Laboratory of the ICTP, Trieste

(Tuniz et al., 2013), according to the following parameters: 110 kV voltage, 90 mA current, angular step of 0.25° over a scan angle of 360°. The final volumes were reconstructed with an isotropic voxel size of 20.6 μm All other specimens were scanned with either a BIR ACTIS 225/300 (130 kV, 100 μA, 0.25 brass filter) or a Skyscan 1172 (100 kV, 94 μA, 2.0 mm aluminum and copper) scanner. Pixel dimensions and slice spacing of the resultant images ranged between 10 and 60 μm. The complete image stack of each tooth was filtered to improve tissue gray-scale homogeneity (Wollny et al., 2013). Filtered image stacks were segmented into enamel and dentine tissues using Avizo/Amira 6.3 (FEI Visualization Sciences Group). Digital surface models (.ply format) of the EDJ were produced in Avizo using the surface generation module.

*2.2. Protoconule expression*

The protoconule is a cuspule mesiobuccal to the protocone, located on the preprotocrista or at the intersection of the preprotocrista and the hypoparacrista (Butler, 1985; Remane, 1960; Szalay, 1969). Protoconule expression at the EDJ was assessed visually by AO using the following scoring system (Fig. 1): Grade 0, protoconule is absent; Grade 1, faint furrows and other irregularities, slight bumps or weak pointed elevations are present; Grade 2, a moderate protoconule is present, and roughly <50% of the height of the protocone from the same tooth. Grade 3: a large protoconule is present, and ≥50% of the height of the protocone from the same tooth as seen from the midpoint of the mesial marginal ridge. Grade 1 is considered the

"suspected" category as per Turner, Nichol, & Scott (1991) and Skinner & Gunz (2010) to include those cases where it was unclear whether or not a poorly developed protoconule was present. Following Skinner & Gunz (2010), most of the "suspected" cases may represent protoconules whose growth initiated but did not progress substantially due to mineralization. This category was further subdivided into grade 1A (bumps and other barely discernible irregularities) and grade 1B (slight pointed elevations that may mark the presence of a dentine horn). The significance of the observed patterns was tested via bootstrapping (1,000 iterations) performed in R 3.4.3 (R Development Core Team, 2017).

The lowest score was chosen when protoconule expression fell at the boundary of two grades. Moreover, when two or more cuspules were present on the preprotocrista, the lingual-most cuspule was scored as the protoconule. To further standardize data collection procedures and minimize error introduced by differences in orientation along the axes and colormap settings, protoconule expression was collected using the following protocol. Each tooth was oriented in occlusal view (i.e., occlusal surface parallel to the xy-plane of the Cartesian coordinate system), with the mesial side of the crown placed at the bottom of the screen. The mesial portion of the longitudinal (mesiodistal) groove was then aligned with the y-axis, and the main buccolingual groove with the x-axis. Once oriented, each tooth was rotated -90 degrees around the local x-axis using the transform editor in Avizo/Amira 6.3 so that the entire mesial aspect of each tooth crown was perpendicular to the xy-plane. A grid was added and color settings of the EDJ models were set to color mode "*boundary ids"* for consistency. Protoconule expression was collected

exclusively on that view, without further manipulation of the virtual models. To test for error in protoconule assessment all teeth were scored twice by AO, with scoring sessions separated by ~1.5 months. The percentage of disagreement between the two sessions was 4.1%, and in all cases, disagreements were never greater than one grade of expression.

While an account of the developmental homology of the protoconule is beyond the scope of our study, we note that assessments of protoconule expression may vary depending on both tooth orientation and dental tissue analyzed. For example, we found cases in which the protoconule were expressed as an expansion of the mesiolingual corner of the tooth along the occlusal surface with minimal height involvement (Fig. S2). Similarly, enamel deposition and the confounding effect of a marked cingulum on the mesiolingual aspect of teeth may lead to score the protoconule as present at the OES (Fig. S3a,b). We also found cases of protoconule presence derived entirely from enamel deposition (i.e., the protoconule is absent at the EDJ, but present at the OES), especially among early hominins (Fig. S3c). It is important to note, however, that there are limitations to the size of structures that can be imaged based on scan resolution, scan parameters and post-processing steps (i.e., one must consider that very small dentine horns could be present but not detectable on the final EDJ model). Even more common are small irregularities and faint bumps on the preprotocrista as observed at the EDJ, with no clear protoconule presence or absence at the OES (Fig. S3d,e). Orientation and the angle from which a tooth is viewed may also lead to ambiguities regarding protoconule presence (Fig. S3f).

Therefore, to minimize potential ambiguities, our study focused exclusively on the EDJ using standardized views, as described above, to record protoconule expression.

*2.3. Geometric morphometric analysis*

We performed a geometric morphometric analysis in order to quantify and visualize group shape differences in the mesial portion of the upper molars between the protocone and paracone that may be associated with protoconule expression (and/or that of other conules). To do so, 3D landmarks and semi-landmarks were digitized on the virtual models of the EDJ using Avizo/Amira 6.3. As illustrated in Fig. 2, landmarks were placed on the tip of the protocone, the midpoint of the mesial marginal ridge and tip of the paracone, and a set of 23 semi-landmarks connecting the three main landmarks were digitized to capture the entire configuration of the mesial portion of the trigon and mesial marginal ridge (hereafter mesial fovea; Harrison & Gu, 1999). Landmark and semi-landmark digitizing was conducted by AO.

Intra-observer error was assessed on 25 randomly selected teeth in which all landmarks and semi-landmarks were digitized twice, with sessions separated by three months. The systematic and random error was tested using repeated measures ANOVA (Anova-RM) and intra-class correlation coefficients (ICC), respectively. Anova-RM tests the hypothesis of no differences between the means of repeated observations under the hypothesis of non-independence, while ICC measures the relationship between the intergroup and intragroup variance. The results of the Anova-RM show that there are non-significant differences between

digitizing sessions (Table S2). Similarly, ICC values reveal a highly significant correlation between sessions (Table S3). Both analyses indicate that intra-observer error is negligible.

Landmark and semi-landmark data were imported to R 3.4.3 using Nat (v.1.8.9; Jefferis and Manton, 2017) and Arothron (Profico and Veneziano, 2015) packages. The R packages Geomorph (Adams et al., 2015) and Morpho (Schlager, Jefferis, & Dryden, 2017), as well as MorphoJ (Klingenberg, 2011) were used for data processing and analyses. Semi-landmarks were slid along their curve by minimizing the bending energy of the thin-plate spline deformation between each specimen and the Procrustes average for the sample (Gunz, Mitteroecker, & Bookstein, 2005). Because we were investigating bilateral structures (i.e., right and left upper molars), a reflection procedure was implemented in order to discard non-relevant right-left differences. We randomly chose to work on right molars, such that all left landmark/semi-landmark configurations were mirror-imaged. After sliding, landmark and semi-landmark configurations were superimposed using a generalized Procrustes analysis to convert them into shape variables. Centroid size calculated from landmark/semi-landmark data was analyzed independently to test for mesial fovea differences attributed exclusively to size. To that end, we conducted Kruskal-Wallis one-way analysis of variance among samples, for each molar type analyzed independently and combined (Table S4). Analyses were performed in Statistica StatSoft 10.0.

Analyses of the Procrustes shape coordinates were performed on M1, M2 and M3 separately and combined via principal component analysis (PCA) and canonic variate analysis

(CVA). When M1-M3 were combined, we also included those molars of uncertain serial position. Due to restrictions in the CVA computation (the number of variables must be smaller than the number of specimens), we reduced the dimensionality of our data by using a subset of principal components (ranging from 15 to 18) explaining 95% of the total shape variation to compute the CVAs. The PCAs and CVAs were conducted in MorphoJ (Klingenberg, 2011) and PAST (Hammer, Harper, & Ryan, 2001). Finally, we used pairwise discriminant function analysis (DFA), as implemented in MorphoJ (Klingenberg, 2011), to investigate mesial fovea shape differences between different group pairs. As it deals with pairwise comparisons, this test differs from the classic CVA in that it allows the calculation and visualization of sample mean differences between pairs. Mahalanobis distances were used to assess the magnitude of the morphological differences between sample means, with significance set at $p < 0.01$.

*2.4. Visualization of mesial fovea shape variation*

We followed two different approaches to visualize mesial fovea shape variation in hominoids. First, we used a method for warping 3D surfaces following Bookstein's (1989) thin plate spline algorithm based on a reference and a target configuration. We used a 3D surface of the mesial fovea of a recent *H. sapiens* as a template to visualize shape deformations along PC and CV axes in all taxa analyzed. The 3D shape deformation analysis was done in R 3.4.3 (R Development Core Team, 2017) using the package Morpho (Schlager et al, 2017). Second,

wireframe graphs were performed in MorphoJ (Klingenberg, 2011) using the pairwise DFA tool. The superimposed wireframes representing mean landmark configurations were depicted using a combination of the 3 axes (1 vs. 2, 1 vs. 3, 2 vs. 3; only the most informative combination – 1 vs. 2 – presented here). Scatterplots were employed to visualize the data point distribution in the multivariate shape space.

### *2.5. Tooth identification of Pleistocene* Pongo *from China and Vietnam*

Tooth type identification of fossil *Pongo* from China was performed by Reiko Kono based on observations of known characteristics for each tooth type, published descriptions of the *Pongo* dentition, and presence of inter-proximal facets (Kono, personal communication). *Pongo* teeth from Vietnam of unknown or ambiguous serial position were assigned to a molar type following a cross-validation approach in which each specimen was considered "unknown" and then classified based on the *Pongo* sample with secure molar identification (M1-3s; unfortunately no microCT scans of extant *Pongo* individuals with M4s were available to include in this analysis). To this end, all 53 upper molars of extant *Pongo* and fossil *Pongo* from China and Vietnam with known serial position were combined in a single sample. For each molar type, we conducted a CVA using the set of principal components that explained 95% of variation in the PCA. Classification accuracy of mesial fovea shape was 82.7% (Fig. S4). Given the high classification accuracy, we used posterior probabilities derived from the CVA to provide a statistically-based classification for the fossil *Pongo* upper molars from Vietnam (Table S5).

**3. Results**

The frequency and expression of the protoconule at the EDJ per molar type and group at different taxonomic levels are summarized in Table S6 and Figs. 3 and S5. Examples of each degree of protoconule expression observed in each taxon are provided in Figs. 4-9 and S6-11. For all molars combined, our dental non-metric analyses reveal that a moderate or large protoconule (i.e., grades 2 or 3) is present in 80% and 86.7% of the Pleistocene and extant *Pongo* individuals, respectively. This is also the case for *Sivapithecus*, as the three specimens examined here presented a grade 2 protoconule. In contrast, moderate to pronounced expressions of the protoconule in hominins, *Meganthropus*, and African great apes occur in low frequencies (0%-14.1% when data are pooled at the genus level, with the greatest frequency seen in *Homo*). In these latter groups, the protoconule is most frequently either absent or weakly expressed (for grades 0 and 1A/1B combined: 95.9% in *Australopithecus*, 95.6% in *Paranthropus*, 85.3% in *Homo*, 100% in *Meganthropus*, 100% in *Pan*, and 100% in *Gorilla*). While sample sizes for early *Homo* and *H. erectus* are small, when the protoconule in *Homo* is examined at the species level, moderate to pronounced expressions were most commonly observed among Pleistocene *H. sapiens* (22.2%) and *H. neanderthalensis* (19.3%).. As illustrated in Figs. 7-8 and S7-8, however, even the greatest degrees of protoconule expression in humans are generally characterized by a small and low but pointed cuspule located more mesially on the preprotocrista. Conversely, the protoconule in *Pongo* tends to be located more lingually than in

humans, closer to the protocone, and its morphology is characterized by either a tall and pointed or broad and blunt tubercle (Figs. 4-6). The bootstrapping analysis (95% confidence) indicates that frequencies of moderate to pronounced protoconules in *Pongo* are significantly different from hominins and African great apes. Differences among species within the Homininae, on the other hand, are nearly always non-significant (Table S7).

Similar results were obtained when each molar type was analyzed independently (rather than combined). Frequencies of moderate to pronounced protoconules (grades 2 and 3) in *Pongo* (including Pleistocene and extant samples) are between 78.4% (M1) and 93.8% (M2). The largest protoconules (grade 3), however, are more frequently found in M1. Grade 3 protoconules were never observed in our *Homo* sample, but moderate or medium-sized (grade 2) expressions were found in 8.6% (M2) to 25% (M1) of the molars. Compared to its metameres, the protoconule is more common and/or strongly expressed in M1 in later *Homo* (including MPEH, *H. neanderthalensis*, and *H. sapiens*); this trend is particularly clear in Pleistocene *H. sapiens*. In contrast, none of the *H. erectus* specimens in our sample exhibited moderate (grade 2) to large (grade 3) protoconule expressions, but an accessory tubercle was observed on the mesial marginal ridge of Sangiran 4 M3 (Fig. 7d). A similar accessory tubercle was also found on both Trinil 11620 and Trinil 11621 (Fig. 9). Grades 2 or 3 of protoconule in the African great apes examined were also rare or absent.

Although only the protoconule was the focus of this study, it is worth noting the high frequency of accessory cuspules and/or tubercles on the mesial marginal ridge and/or

preparacrista of human molars (Fig. S12), especially in *Homo sapiens* (83.3% and 71.4% of the Pleistocene and recent *H. sapiens* examined, respectively), followed by *H. neanderthalensis* (52.6%) and *H. erectus* (28.6%). *Pongo* also exhibits a relatively high frequency of accessory cuspules and/or tubercles (extant *Pongo*: 30%, Pleistocene *Pongo* from China: 48%, Pleistocene *Pongo* from Vietnam: 54%) in addition to the protoconule, whereas they occur in low frequencies in early hominins (0%-6.7%) and African great apes (0%-3.5 %). The way these cuspules are expressed, however, generally differ between *Homo* and *Pongo*. When present, *Homo* tends to exhibit multiple accessory cuspules and/or tubercles along the mesial marginal ridge. *Pongo*, on the other hand, tends to have only one accessory cuspule and/or tubercle on the mesial marginal ridge (Pleistocene *Pongo* from China and extant *Pongo*) or preparacrista (Pleistocene *Pongo* from Vietnam). Our *Sivapithecus* and *Megathropus* samples are too small to draw conclusions on the pattern of mesial marginal tubercles in these taxa.

For the mesial fovea, the results of the CVA performed on M1, M2 and M3 separately and combined show that Pleistocene *Pongo* from China and Vietnam and extant *Pongo* cluster together, even if they were treated as separate groups for analyses (Figs. 10 and S17-19; see also Figs. S13-16 for PCA). In most cases, *Pongo* is also clearly differentiated from all members of *Homo*, *Australopithecus, Paranthropus*, *Meganthropus, Pan* and *Gorilla*. As illustrated in Fig. 10 for all molars combined, *Pongo* and *Homo* occupy opposite sides along the first canonical axis, while the greatest (but still minor) overlap of the *Pongo* samples occur with *Australopithecus* and *Paranthropus*. Interestingly, *Sivapithecus* occupies an area in morphospace

where the overlap among *Pongo*, *Australopithecus*, and *Paranthropus* takes place. It is also worth noting the high degree of overlap in mesial fovea shape between the M1 of *Paranthropus* and all species of *Homo* (except for *H. erectus*) (Fig. S17). This degree of overlap, however, does not hold true for M2 and M3. Overall, mesial fovea shape possesses a high classification accuracy, reaching ~72%-85% when all teeth are analyzed together and between ~91%-95% when each molar type is analyzed independently (Table 2). Interestingly, the variation in mesial fovea for M3 appears to be particularly high among members of the genus *Homo* (Fig. S19).

When multivariate techniques are performed exclusively on *Homo* and *Pongo*, PCA and CVA results for all molars combined also show a clear separation between the two genera (Figs. 11 and S20-26). While all species of *Homo* cluster together and occupy the negative side along the first canonical axis, our three samples of *Pongo* are located on the positive side of this first axis. As summarized in Table S8, classification accuracy for the species included in the two genera reaches ~88% (all molar types included). Although correct taxonomic classification is slightly higher when each molar type is analyzed independently (between 88%-92%), the position of early *Homo* along the first canonical axis relative to other hominoid taxa is slightly more ambiguous. That is, M1 mesial fovea shape of *H. erectus s.l.* occupies an intermediate position between *Pongo* and the other *Homo* samples analyzed. Although our early *Homo* sample overlaps with *H. sapiens* in M1 mesial fovea shape, that of M2 and M3 makes early *Homo* cluster closely with *Pongo*. The M2 and M3 of *H. erectus s.l.*, however, show closer affinities with later *Homo* in mesial fovea shape (Figs. S24-26).

The results of the pairwise DFAs, performed to compare group means in mesial fovea shape, are illustrated in Fig. 12. Our results show that extant and fossil *Pongo* have a similar mesial fovea shape and only subtle differences can be observed, such as the slightly sharper, more pronounced and buccally oriented protoconule in extant *Pongo.* The shape of the mesial marginal ridge of both Pleistocene and extant *Pongo* is similar, although it is slightly more expansive mesially in the fossil group. When *Pongo* and humans (with *H. erectus s.l.* analyzed both independently and as part of the genus *Homo*) are compared, differences in mesial fovea shape become evident. The protocone is more peripherally positioned in *Pongo* and a pointed and strongly developed protoconule tubercle is present on the preprotocrista. Both the mesial marginal ridge and the protoconule also tend to be more mesially positioned in *Pongo* compared to *Homo*. The mean shape of the mesiolingual aspect of human upper molars reveals no traces of a protoconule. Human molars, however, exhibit a mesiobuccal expansion of the buccal portion of the mesial marginal ridge and an overall increase in the surface area of the paracone relative to the protocone. There are no major differences between *Pongo* and humans in the position of the paracone cusp apex along the mesiodistal and buccolingual planes. However, height differentials between the protocone and paracone apices are more pronounced in *Pongo* teeth, which show a notably lower protocone relative to the paracone. Overall, humans possess higher-cusped crowns and a concomitantly relatively deep and broad mesial fovea.

**4. Discussion**

More than 100 years ago, Selenka (1898) identified the common presence of the protoconule among extant *Pongo*, including both males and females. Reported frequencies were 90% (males) and 76% (females) for M1, 100% (males) and 94% (females) for M2, and 100% (males) and 93% (females) for M3, suggesting that the protoconule is slightly more common in males (vs. females) and in M2 and M3 (vs. M1). Hooijer (1948), in his comprehensive study of orangutan dental remains from Quaternary deposits in Sumatra, reported similar results for fossil *Pongo*, where frequencies of protoconule expression range between 88% (M1 and M3) and 90% (M2). He also noted a high incidence (85%-100%) of the protoconule in his comparative sample of recent *Pongo*. Our results of the presence of the protoconule at the EDJ of *Pongo* teeth are consistent with these earlier observations. We found that the M2 is the most common tooth of the upper molar row exhibiting the protoconule. When present, however, the protoconule appears to be more strongly expressed in M1.

While neither Selenka (1898) nor Hooijer (1948) examined patterns of protoconule expression in other great apes, subsequent observations (Delson & Andrews, 1975; Korenhof, 1960; Swindler, 1976; Swindler & Olshan, 1988; Pilbrow, 2003) revealed that this cuspule occurs much less frequently in *Pan* and *Gorilla*. This appears to be particularly true in *Pan*, as the protoconule in this genus is generally "barely distinguished" according to Swindler & Olshan (1988: 277). *Gorilla* occupies an intermediate position between *Pan* and *Pongo* in protoconule incidence and degree of expression. Our data support these claims, but the results differ from a large-scale study by Pilbrow (2003) on the African great ape dentition. Contrary to our results

and those reported elsewhere (Korenhof, 1960; Swindler, 1976; Swindler & Olshan, 1988), Pilbrow (2003) identified relatively high frequencies of protoconule expression in *Pan* (M1: 33%-66%, M2: 33%-66%, M3: 15%-45%, depending on the species and subspecies sampled). No frequency data for the protoconule in *Gorilla* were reported but given that Pilbrow's (2003) sample size was much larger than that used here or elsewhere, it is likely that these inconsistencies are the product of sampling error and the different dental tissues examined. Overall, however, even using Pilbrow's (2003) data, *Pan* has a rarer occurrence of the protoconule relative to *Pongo*.

The protoconule is a commonly used character in reconstructions of the evolutionary relationships of catarrhine primates (e.g., Alba et al., 2015; Delson & Andrews, 1975; Harrison, 1987; Nengo et al., 2017; Rossie & MacLatchy, 2006; Stevens et al., 2013). As noted above, the ancestral catarrhine and hominoid morphotypes would have included the presence of a protoconule as a common feature of the upper molars (Delson & Andrews, 1975; Harrison, 1987). Our results show that *Pongo* exhibits the ubiquitous presence of a large protoconule, while this cuspule in *Pan* and *Gorilla* occurs much less frequently and is more weakly expressed. Although our *Sivapithecus* sample is small, the morphology and frequency of the protoconule present in this extinct taxon closely approximates those of *Pongo*, which further strengthen the long-held view regarding the close relationship between the two taxa. In hominins the protoconule is either lost or reduced; in the latter case, the protoconule is generally expressed as a small but pointed cuspule. *Homo neanderthalensis* and *H. sapiens* also exhibit a multiplication

of conules along the preprotocrista and the mesial marginal ridge. Given these findings, *Pongo* can be inferred to have retained the primitive catarrhine and hominoid condition, while hominines (i.e., African apes and hominins) are derived in having protoconules that occur less frequent and are relatively less well-developed.

Our multivariate analyses also revealed the distinctive mesial fovea shape of *Pongo* upper molars compared to those of *Homo* and other hominids. While these analyses suggest that shape variation of the mesial fovea is higher in *Homo* than in *Pongo*, we caution that this could be an artifact of the larger number of individuals from the genus *Homo* used in our study. Compared to *H. erectus s.l.* and the genus *Homo* as a whole, both Pleistocene and recent *Pongo* molars exhibit, on average, a marginalized protocone with a marked protoconule on the preprotocrista and greater height differentials between a relatively low protocone and tall paracone. This pattern in *Pongo* is consistent across a temporo-spatially diverse sample of individuals, despite the high degree of variation in other dental morphological features documented among members of this genus (Harrison, 2000; Harrison et al., 2014; Schwartz et al., 1995; Uchida, 1996, 1998; Tshen, 2016). However, an interesting characteristic of Pleistocene *Pongo* from Vietnam is the regular presence of a small tubercle on the preparacrista in addition to the protoconule; this was rarely observed in fossil *Pongo* from China and our sample of extant orangutans. Using a large dataset, Smith et al. (2011) and Smith (2016) also reported that Pleistocene *Pongo* has slightly higher average enamel thickness, especially in upper and lower M1, but that cuspal enamel thickness does not differ between Pleistocene and extant *Pongo*. They also noted that while both groups

exhibit similar long-period line periodicity values, fossil *Pongo* teeth have a higher number of lines and thus slightly lower extension rates.

The results of this study suggest that the protoconule (and overall morphology of the mesial fovea) is a potentially useful feature for the taxonomic identification of isolated hominid teeth found in Pleistocene deposits of Asia, especially when dental wear has obliterated diagnostic features at the external enamel surface. We caution, however, that, because of the degree of morphological overlap and the fact that this variant is not unique to *Pong*o, this feature cannot be used in isolation. Instead, the mesial fovea shape and presence of a well-developed protoconule should be used in combination with other diagnostic features for accurate taxonomic assessments. Previous studies of tooth microstructure and dental tissue proportions have identified additional dental features that differ between pongines and hominins, such as the equal reduction of enamel and dentine in *Pongo*, but preferential loss of dentine in *Homo* during the process of tooth size reduction in these two groups (Grine & Franzen, 1994; Smith et al., 2011; with the exception of Neanderthals, see Olejniczak et al., 2008b). *Pongo* molars also differ from those of humans in having lower dentine horns and an overall different shape of the EDJ with broader crowns, broad and shallow dentinal intercuspal furrow pattern and less medially placed lingual dentine tips (Olejniczak, Martin, & Ulhaas, 2004; Olejniczak et al., 2008a; Smith et al., 2018; Zanolli et al., 2019). In addition, when only fossil individuals were considered, Smith et al. (2012) found that enamel has a more uniform distribution across the enamel cap in fossil *Pongo* than in *H. erectus*, although relative enamel thickness values overlap substantially in the two taxa

(Smith et al., 2018). However, when only extant members of *Pongo* and *Homo* were considered and analyzed in 3D (i.e., the entire crown) rather than 2D cross sections, Kono (2004) noted that while *Pongo* exhibited relatively thicker occlusal but thinner basal enamel, molar enamel in *Homo* was relatively thicker throughout the crown. Long-period line periodicity is also significantly higher in Pleistocene *Pongo* than in *Homo*, resulting in longer crown formation times in the former group (Rong, LingXia, & XinZhi, 2012; Smith et al., 2012; Smith, 2016; Smith et al., 2018). The feasibility to collect some of these data, however, is highly contingent on dental wear. Given the growing access to micro-computed tomographic facilities, reduced dependency on the need of unworn teeth, and ubiquitous presence of the protoconule in *Pongo* molars irrespective of their position in the molar row, we highlight the discriminatory power carried by this feature for differentiating *Pongo* from *Homo*. Thus, our results provide a morphological feature that may prove useful in helping to resolve ambiguities in cases where the taxonomic identification of Asian hominoid dental remains has proven problematic. This is an issue of paramount importance, because in order to document the spatial and temporal distribution of hominins and *Pongo* in the Pleistocene of Asia it is crucial to have a high degree of confidence in taxonomic attributions. The morphological features discussed here can be used as part of a suite of diagnostic dental traits to help determine the taxonomic identity of isolated and worn hominoid upper molars from the Pleistocene of Asia.

**Acknowledgments**

For access to specimens, we thank the following institutions: Croatian Museum of Natural History, Croatia; Ditsong National Museum of Natural History, South Africa; Francisc Rainer Anthropology Institute, Romania; National Museums of Kenya, Kenya; Musée d'Art et d'Archéologie du Périgord, Framce; Musée d'Archéologie Nationale de Saint-Germain-en-Laye, France; Musée d'Angoulême, France; Musée National de Préhistoire des Eyzies, France; Musée de l'Homme, France; Museo Nacional de Ciencias Naturales, Spain; Max Planck Institute for Evolutionary Anthropology, Germany; Royal Museum for Central Africa, Belgium; Museum für Vor und Frühgeschichte, Germany; National Museum of Ethiopia, Museum National d'Histoire Naturelle, France; American Museum of Natural History, USA; Rockefeller Museum, Israel; Royal Belgian Institute of Natural Sciences, Belgium; Senckenberg Research Institute, Germany; Sackler School of Medicine, Israel; Smithsonian National Museum of Natural History, USA; Center for the Study of Human Origins at New York University, USA; Tel Aviv University, Israeil; Leipzig University, Germany; University of Witwatersrand, South Africa; Direction du Patrimoine Culturel and Musée Archéologique de Rabat, Morocco. We also thank Colin Menter, Bill Kimbel, Jay Kelley, Friedemann Schrenck, and Ottmar Kullmer for access to material. We thank Heiko Temming, David Plotzki, Lukas Westphal, Kornelius Kupczik, Ellis Locke, and Susan Antón for help and comments. For technical help with the microCT scanning of the *Sivapithecus* specimens, we thank Federico Bernardini and Claudio Tuniz. This research was supported by the National Science Foundation (award number: 1341148), the Wenner-Gren Foundation, the Leakey Foundation, and the NYU GSAS James Arthur Fellowship (grants to

AO). Scanning of the Vietnamese *Pongo* specimens was funded to Anne-Marie Bacon by the PICS-CNRS. Scanning of the fossil hominins was supported by the Max Planck Society.



**Data availability statement**

The data that support the findings of this study are available on request from the corresponding author. The data are not publicly available due to previous agreements with participating institutions.

**References**

Adams, D.C., & Otárola-Castillo, E. (2013). Geomorph: an r package for the collection and analysis of geometric morphometric shape data. *Methods in Ecology and Evolution*, 4, 393-399.

Alba, D.M., Moyà-Solà, S., Malgosa, A., Casanovas-Vilar, I., Robles, J.M., Almécija, S., Galindo, J., Rotgers, C., Mengual, J.V.B. (2010). A new species of *Pliopithecus* Gervais, 1849 (Primates: Pliopithecidae) from the Middle Miocene (MN 8) of Abocador de Can Mata (els Hostalets de Pierola, Catalonia, Spain). *American Journal of Physical Anthropology,* 141, 52-75.

Alba, D.M., Moyà-Solà, S., Robles, J.M., & Galindo, J. (2012). The oldest pliopithecid record in the Iberian Peninsula based on new material from the Vallès-Penedès Basin. *American Journal of Physical Anthropology,* 147, 135-140.

Alba, D. M., Almécija, S., Demiguel, D., Fortuny, J., Pérez de los Ríos, M., Pina, M., Robles, J. M., & Moyà-Solà, S. (2015). Miocene small-bodied ape from Eurasia sheds light on hominoid evolution. *Science,* 350, aab2625.

Andrews, P. (1978). A revision of the Miocene Hominoidea of East Africa. *Bulletin of the British Museum (Natural History), Geology Series,* 30, 85-225.

Antón, S.C. (2003). The natural history of *Homo erectus*. *American Journal of Physical Anthropology,* S37, 126-170.

Ao, H., Dekkers, M. J., Wei, Q., Qiang, X. K., & Xiao, G. Q. (2013). New evidence for early presence of hominids in north China. *Scientific Reports,* 3, 2403.

Bacon, A.-M., & Long, V. T. (2001). The first discovery of a complete skeleton of a fossil orang-utan in a cave of the Hoa Binh Province, Vietnam. *Journal of Human Evolution,* 41, 227-241.

Bacon, A.-M., & Long, V. T. (2002). *Erratum*: The first discovery of a complete skeleton of a fossil orang-utan in a cave of the Hoa Binh Province, Vietnam. *Journal of Human Evolution,* 42, 505.

Bacon, A.-M., Demeter, F., Duringer, P., Helm, C., Bano, M., Vu, T. L., Nguyen, T. K. T., Antoine, P.-O., Bui, T. M., Nguyen, T. M. H., Dodo, Y., Chabaux, F., & Rihs, S. (2008). The Late Pleistocene Duoi U'Oi Cave in northern Vietnam: Palaeontology, sedimentology, taphonomy and palaeoenvironments. *Quaternary International Reviews,* 27, 1627-1654.

Begun, D.R. (1992). *Dryopithecus crusafonti* sp. nov., a new Miocene hominoid species from Can Ponsic (northeastern Spain). *American Journal of Physical Anthropology,* 87, 291-309.

Bergstrom, K., Jenkins, K., Levy, J., Velasquez, R.J., Lewis, P.J., & Campbell, T.L. (2016, April). Computed tomography survey of supernumerary molars in extant orangutans with implications for studies of the primate fossil record. Paper presented at the Paleoanthropology Society 2016 Meeting, Atlanta. GA. PaleoAnthropology Abstracts, A4.

Bookstein, F.L. (1989). Principal Warps: Thin-plate splines and the decomposition of deformations. *IEEE Transactions on pattern analysis and machine intelligence,* 11, 567-585.

Bown, T.M., & Kraus, M.J. (1979). Origin of the tribosphenic molar and the metatherian and eutherian dental formulae. In J.A. Lillegraven, Z. Kielan-Jaworowska, & W.A. Clemens (Eds.), *Mesozoic mammals: The first two-thirds of mammalian history* (pp. 172-181). Berkeley, University of California Press.

Butler, P. M. (1956). The ontogeny of molar pattern. *Biological Reviews of the Cambridge Philosophical Society,* 31, 30-69.

Butler, P.M. (1978). Molar cusp nomenclature and homology. In P.M. Butler and K.A. Joysey (Eds.), *Development Function and Evolution of Teeth* (pp. 439-453). New York, NY: Academic Press.

Butler, P. M. (1985). Homologies of molar cusps and crests, and their bearing on assessments of rodent phylogeny. In W. P. Luckett, & J. L. Hartenberger (Eds.), *Evolutionary Relationships among Rodents* (pp. 381-401). New York, NY: Plenum Press.

Butler, P.M. (1992). Tribosphenic molars in the Cretaceous. In P. Smith, & E. Tchernov (Eds.), *Structure, Function and Evolution of Teeth* (pp. 125-138). Tel Aviv: Freund Publishing House.

Ciochon, R. L. (2009). The mystery ape of Pleistocene Asia. *Nature,* 459, 910-911.

Ciochon, R. L. (2010). Divorcing hominins from the Stegodon-Ailuropoda fauna. New views on the antiquity of hominins in Asia. In J. G. Fleagle, J. J. Shea, F. E. Grine, A. L. Baden, & R. E. Leakey (Eds.), *Out of Africa I: The First Hominin Colonization of Eurasia* (pp. 111-126). New York, NY: Springer.

Ciochon, R. L., Olsen, J. W., & James, J. (1990). *Other origins: The search for the giant ape in human prehistory.* New York, NY: Bantam Books.

Cote, S., McNulty, K.P., Steven, N.J., & Nengo, I.O. (2016). A detailed assessment of the maxillary morphology of *Limnopithecus evansi* with implications for the taxonomy of the genus. *Journal of Human Evolution,* 94, 83-91.

Crompton, A.W. (1971). The origin of the tribospenic molar. In D.A.Kermack & K.A. Kermack (Eds.), *Early Mammals* (pp. 65-87). London: Academic Press.

Delson, E., & Andrews, P. (1975). Evolution and interrelationships of the catarrhine primates. In W. P. Luckett, & F. S. Szalay (Eds.), *Phylogeny of the Primates: A Multidisciplinary Approach* (pp.405-446). New York: Plenum Press.

Delson, E., & Rosenberger, A.L. (1984), Are there any anthropoid primate living fossils? In N. Eldredge & S.M. Stanley (Eds.), *Living Fossils* (pp. 50-61). New York: Springer.

Demeter, F., Bacon, A.-M., Nguyen, K. T., Long, V. T., Matsumura, H., Ha, H. N., Schuster, M., Nguyen, M. H., & Coppens, Y. (2004). An archaic *Homo* molar from Northern Vietnam. *Current Anthropology,* 45, 535-541.

Drawhorn, G. M. (1995). *The systematics and paleodemography of fossil orangutans (genus* Pongo*)* (Unpublished doctoral dissertation). University of California, Davis, California, USA.

de Vos, J. (2004). The Dubois collection: a new look at an old collection. In C. F. Winkler Prins, & S. K. Donovan (Eds.), *VII International Symposium Cultural Heritage in Geosciences, Mining and Metallurgy* (pp. 267–285). Leiden, Netherlands: Scripta Geologic.

Etler, D. A., Crummett, T. L., & Wolpoff, M. H. (2001). Longgupo: Early *Homo* colonizer or Late Pliocene *Lufengpithecus* survivor in South China? *Human Evolution,* 16, 1-12.

Falguères, C., Sémah, F., Saleki, H., Hameau, S., Tu, H., Féraud, G., Simanjuntak, H., & Widianto, H. (2016). Geochronology of early human settlements in Java: What is at stake? *Quaternary International,* 416, 5-11.

Garn, S. M, Lewis, A. B., & Kerewsky, R. S. (1963). Molar size sequences and fossil taxonomy. *Science,* 142, 1060.

Godinot, M. (1994). Early North African primates and their significance for the origin of Simiiformes (=Anthropoidea). In J. G. Fleagle, & R. F. Kay (Eds.), *Anthropoid Origins* (pp. 235-295). New York, NY: Springer.

Goose, D. H. (1963). Dental measurement: an assessment of its value in anthropological studies. In D. R. Brothwell (Ed.), *Dental Anthropology* Vol. V (pp. 125-148). London, UK: Pergamon Press.

Grine, F., & Franzen, J. L. (1994). Fossil hominid teeth from the Sangiran Dome (Java, Indonesia). *Courier Forschungsinstitut Senckenberg,* 171, 75-103.

Groves, C., 2001. *Primate taxonomy.* Washington, DC: Smithsonian Institution Press.

Gunz, P., Mitteroecker, P., & Bookstein, F. L. (2005). Semilandmarks in three dimensions. In D. E. Slice (Ed.), *Modern Morphometrics in Physical Anthropology* (pp. 73-98). New York, NY: Kluwer Academic/Plenum Publishers.

Hammer, Ø., Harper, D. A. T., & Ryan, P. D. (2001). PAST: Paleontological statistics software package for education and data analysis. *Palaeontologica Electronica,* 4, 1-9.

Han, F., Bahain, J.-J., Boeda, E., Hou, Y. M., Huang, W. B., Falguères, C., Rasse, M., Wei, G. B., Garcia, T., Shao, Q. F., & Yin, G. M. (2012). Preliminary results of combined ESR/U-series dating of fossil teeth from Longgupo Cave, China. *Quaternary Geochronology,* 10, 436-442.

Hanegraef, H., Martinón-Torres, M., Martínez de Pinillos, M., Martín-Francés, L., Vialet, A., Arsuaga, J.L., & Bermúdez de Castro, J.M. (2018). Dentine morphology of Atapuerca-Sima de los Huesos lower molars: Evolutionary implications through three-dimensional geometric morphometric analysis. *American Journal of Physical Anthropology*, 166, 276-295.

Harrison, T. (1982). Small-bodied apes from the Miocene of East Africa (Unpublished doctoral dissertation). University of London, London, United Kingdom.

Harrison, T. (1986). New fossil anthropoids from the middle Miocene of East Africa and their bearing on the origin of the Oreopithecidae. *American Journal of Physical Anthropology,* 71, 265-284.

Harrison, T. (1987). The phylogenetic relationships of the early catarrhine primates: A review of the current evidence. *Journal of Human Evolution,* 16, 41-80.

Harrison, T. (1988). A taxonomic revision of the small catarrhine primates from the early Miocene of East Africa. *Folia Primatologica,* 50, 59-108.

Harrison, T. (1998). Vertebrate faunal remains from Madai Caves (MAD 1/28), Sabah, East Malaysia. *Bulletin of the Indo-Pacific Prehistory Association,* 17, 85-92.

Harrison, T. (2000). Archaeological and ecological implications of the primate fauna from prehistoric sites in Borneo. *Bulletin of the Indo-Pacific Prehistory Association,* 20, 133-146.

Harrison, T. (2002). Late Oligocene to middle Miocene catarrhines from Afro-Arabia. In W.C.

Hartwig (Ed.), *The Primate Fossil Record* (pp. 311-338). Cambridge, United Kingdom: Cambridge University Press.

Harrison, T. (2010). Dendropithecoidea, Proconsuloidea, and Hominoidea. In L. Werdelin & W.J. Sanders (Eds.), *Cenozoic Mammals of Africa* (pp. 429-469). Berkeley: University of California Press.

Harrison, T., Delson, E., & Jian G. (1991) A new species of *Pliopithecus* from the middle Miocene of China and its implications for early catarrhine zoogeography. *Journal of Human Evolution,* 21, 329-361.

Harrison, T., & Gu, Y. (1999). Taxonomy and phylogenetic relationships of early Miocene catarrhines from Sihong, China. *Journal of Human Evolution*, 37, 225-277.

Harrison, T., van der Made, J., & Ribot, F. (2002). A new middle Miocene pliopithecid from Sant Quirze, northern Spain. *Journal of Human Evolution,* 42, 371-377.

Harrison, T., Krigbaum, J., & Manser, J. (2006). Primate biogeography and ecology on the Sunda Shelf Islands: a paleontological and zooarchaeological perspective. In S. M. Lehman, J. G. Fleagle (Eds.), *Primate Biogeography* (pp. 331-372). New York, NY: Springer.

Harrison, T., & Andrews, P. (2009). The anatomy and systematic position of the early Miocene proconsulid from Meswa Bridge, Kenya. *Journal of Human Evolution,* 56, 479-496.

Harrison, T., Jin, C., Zhang, Y., & Wang, Y. (2014). Fossil *Pongo* from the early Pleistocene *Gigantopithecus* fauna of Chongzuo, Guangxi, southern China. *Quaternary International,* 354, 59-67.

Hooijer, D. A. (1948). Prehistoric teeth of man and of the orang-utan from central Sumatra, with notes on the fossil orang-utan from Java and southern China. *Zoologische Mededelingen,* 29, 175-301.

Ibrahim, Y. K., Tshen, L. T., Westaway, K. E., Cranbrook, E., Humphrey, L., Muhammad, R. F., Zhao, J.-X., & Peng, L. C. (2013). First discovery of Pleistocene orangutan (*Pongo* sp.) fossils in Peninsular Malaysia: biogeographic and palaeoenvironmental implications. *Journal of Human Evolution,* 65, 770-797.

Ishida, H., & Pickford, M. (1997). A new late Miocene hominoid from Kenya: *Samburupithecus kiptalami* gen. et sp. nov. *Comptes Rendus de l'Académie des Sciences Paris, Sciences de la Terre et des Planètes,* 325, 823-829.

Jefferis, G., & Manton, J. (2017). *Nat: NeuroAnatomy Toolbox for Analysis of 3D Image Data*. R package version 1.8.11.

Kaifu, Y., Fachroel, A., & Baba, H. (2001). New evidence of the existence of *Pongo* in the Early/Middle Pleistocene of Java. *Geological Research and Development Center Special Publication,* 27, 55-60.

Kanazawa, E., Seikikawa, M., & Ozaki, T. (1990). A quantitative investigation of irregular cuspules in human maxillary permanent molars. *American Journal of Physical Anthropology,* 83, 173-180.

Kay, R. F. (1980). Platyrrhine origins: a reappraisal of the dental evidence. In: R. S. Ciochon, & A. B. Chiarelli (Eds.), *Evolutionary Biology of the New World Monkeys and Continental Drift* (pp. 159-188). New York, NY: Plenum Press.

Klingenberg, C. P. (2011). MorphoJ: an integrated software package for geometric morphometrics. *Molecular Ecology Resources* 11, 353-357.

Kono, R. (2004). Molar enamel thickness and distribution patterns in extant great apes and humans: new insights based on a 3-dimensional whole crown perspective. *Anthropological Science*, 112, 121-146.

Kordos, L., & Begun, D.R. (1997). A new reconstruction of RUD 77, a partial cranium of *Dryopithecus brancoi* from Rudabánya, Hungary. *American Journal of Physical Anthropology,* 103, 277-294.

Korenhof, C.A.W. (1960). Morphogenetical aspects of the human upper molar. Utrecht: Uitgeversmaatschappij Neerlandia.

Kunimatsu, Y., Ishida, H., Nakatsukasa, M., Nakano, Y., Sawada, Y., & Nakayama, K. (2004). Maxillae and associated gnathodental specimens of *Nacholapithecus kerioi*, a large-bodied hominoid from Nachola, northern Kenya. *Journal of Human Evolution,* 46, 365-400.

Larick, R., Ciochon, R.L., Zaim, Y., Sudijono, Suminto, Rizal, Y., Aziz, F., Reagan, M., & Heizler, M. (2001). Early Pleistocene $^{40}Ar/^{39}Ar$ ages for Bapang Formation hominins, Central Jawa, Indonesia. *Proceedings of the National Academy of Sciences* USA, 98, 4866-4871.

Le Gros Clark, W.E., & Leakey, L.S.B. (1951). The Miocene Hominoidea of East Africa. *Fossil Mammals of Africa, No. 1. British Museum (Natural History), London*, 1-117.

Macchiarelli, R., Bondioli, L., Debénath, A., Mazurier, A., Tournepiche, J.-F., Birch, W., & Dean, M. C. (2006). How Neanderthal molar teeth grew. *Nature*, 444, 748-751.

Macchiarelli, R., Bondioli, L., & Mazurier, A. (2008). Virtual dentitions: touching the hidden evidence. In J.D. Irish & G.C. Nelson (Eds.), *Technique and Application in Dental Anthropology* (pp. 426-448). Cambridge, United Kingdom: Cambridge University Press.

Macchiarelli, R., Bayle, P., Bondioli, L., Mazurier, A., & Zanolli, C. (2013). From outer to inner structural morphology in dental anthropology: Integration of the third dimension in the visualization and quantitative analysis of fossil remains. In G.R. Scott & J.D. Irish (Eds.), *Anthropological Perspectives on Tooth Morphology: Genetics, Evolution*, Variation (pp. 250-277). New York: Cambridge University Press.

Mahler, P. E. (1973). *Metric variation in the pongid dentition* (Unpublished doctoral dissertation) University of Michigan, Ann Arbor, Michigan, USA.

Marivaux, L., Adnet, S., Altamirano-Sierra, A.J., Boivin, M., Pujos, F., Ramdarshan, A., Salas-Gismondi, R., Tejada-Lara, J.V., & Antoine, P.-O. (2016). Neotropics provides insights

into the emergence of New World monkeys: New dental evidence from the late Oligocene of Peruvian Amazonia. *Journal of Human Evolution,* 97, 159-175.

Martin, L. B. (1985). Significance of enamel thickness in hominoid evolution. *Nature,* 314, 260-263.

Molnar, S. (1971). Human tooth wear, tooth function and cultural variability. *American Journal of Physical Anthropology,* 34, 27-42.

Nater, A., Mattle-Greminger, M. P., Nurcahyo, A., Nowak, M. G., de Manuel, M., Desai, T., Groves, C., Pybus, M., Sonay, T. B., Roos, C., Lameira, A. R., Wich, S. A., Askew, J., Davila-Ross, M., Fredriksson, G., de Valles, G., Casals, F. Prado-Martinez, J., Goossens, B., Verschoor, E. J., Warren, K. S., Singleton, I., Marques, D. A., Pamungkas, J., Perwitasari-Farajallah, D., Rianti, P., Tuuga, A., Gut, I. G., Gut, M., Orozco-terWengel, P., van Schaik, C. P., Bertranpetit, J., Anisimova, M., Scally, A., Marques-Bonet, T., Meijaard, E., & Krützen, M. (2017). Morphometric, behavioral, and genomic evidence for a new orangutan species. *Current Biology,* 27, 1-12.

Nengo, I., Tafforeau, P., Gilbert, C.C., Fleagle, J.G., Miller, E.R., Feibel, C., Fox, D.L., Feinberg, J., Pugh, K.D., Berruyer, C., Mana, S., Engle, Z., & Spoor, F. (2017). New infant cranium from the African Miocene sheds light on ape evolution. *Nature,* 548, 169-174.

Nisbett, R. A., & Ciochon, R. L. (1993). Primates in northern Viet Nam: a review of the ecology and conservation status of extant species, with notes on Pleistocene localities. *International Journal of Primatology,* 14, 765-795.

Olejniczak, A. J., Martin, L. B., & Ulhaas, L. (2004). Quantification of dentine shape in anthropoid primates. *Annals of Anatomy*, 186, 479-485.

Olejniczak, A. J., Smith, T. M., Wang, W., Potts, R., Ciochon, R., Kullmer, O., Schrenk, F., & Hublin, J.-J. (2008a). Molar enamel thickness and dentine horn height in *Gigantopithecus blacki*. *American Journal of Physical Anthropology,* 135, 85-91.

Olejniczak, A.J., Smith, T.M., Feeney, R.N.M., Macchiarelli, R., Mazurier, A., Bondioli, L., Rosas, A., Fortea, J., de la Rasilla, M., Garcia-Tabernero, A., Radovčić, J., Skinner, M.M., Toussaint, M., & Hublin, J.-J. (2008b). Dental tissue proportions and enamel thickness in Neandertal and modern human molars. *Journal of Human Evolution*, 55, 12-23.

Olsen, J. W., & Ciochon, R. L. (1990). A review of evidence for postulated Middle Pleistocene occupations in Viet Nam. *Journal of Human Evolution,* 19, 761-788.

Ortiz, A., Bailey, S.E., Hublin, J.-J., & Skinner, M.M. (2017). Homology, homoplasy, and cusp variability at the enamel-dentine junction of hominoid molars. *Journal of Anatomy,* 231, 585-599.

Pérez de los Rios, M. (2014). *The craniodental anatomy of Miocene apes from the Vallès-Penedès Basin (Primates: Hominidae): Implications for the origin of extant great apes*

(Unpublished doctoral dissertation). Universitat Autònoma de Barcelona, Barcelona, Spain.

Pickford, M.L. (1985). A new look at *Kenyapithecus* based on recent discoveries in western Kenya. *Journal of Human Evolution,* 14, 113-143.

Pilbeam, D.R. (1969). Tertiary Pongidae of East Africa: Evolutionary relationships and taxonomy. *Bulletin of the Peabody Museum of Natural History,* 31, 1-185.

Pilbeam, D.R., Rose, M.D., Badgley, C., Lipschutz, B. (1980). Miocene hominoids from Pakistan. *Postilla,* 181, 1-94.

Pilbrow, V. C. (2003). *Dental variation in African apes with implications for understanding patterns of variation in fossil apes* (Unpublished doctoral dissertation). New York University, New York, NY, USA.

Pilbrow, V.C. (2018). Dental diversity in *Pongo* as revealed by molar occlusal morphometrics. *American Journal of Physical Anthropology,* S66, 208.

Profico, A., & Veneziano, A. (2015). *Arothron: R functions for geometric morphometric analyses*. R package version 314 1.1.

R Core Team (2017). *R foundation for statistical computing*. Vienna, Austria. Version 3.4.3. Available from: http://www.R-project.org.

Remane, A. (1960). Zahne und Gebiss. *Primatologia III*. Basel, Switzerland: Karger.

Rong, H., LingXia, Z., & XinZhi, W. (2012). Periodicity of Retzius lines in fossil *Pongo* from South China. *Chinese Science Bulletin*, 57, 790-794.

Rossie, J.B., & MacLatchy, L. (2006). A new pliopithecoid genus from the early Miocene of Uganda. *Journal of Human Evolution,* 50, 568-586.

Schlager, S., Jefferis G., & Dryden, I. (2017). Morpho: Calculations and visualisations related to geometric morphometrics. R package version 2.6

Schour, I., & Massler, M. (1940). Studies in tooth development. The growth pattern of the human teeth. *The Journal of the American Dental Association,* 27, 1778-1793, 1918-1931.

Schuman, E. L. & Brace, C. L. (1954). Metric and morphologic variations in the dentition of the Liberian chimpanzee: comparisons with anthropoid and human dentitions. *Human Biology,* 26, 239-268.

Schwartz, J.H, & Tattersall, I. (1985). Evolutionary relationships of living lemurs and lorises (Mammalia, Primates) and their potential affinities with European Eocene Adapidae. *Anthropological Papers of the American Museum of Natural History,* 60, 1-100.

Schwartz, J. H., & Tattersall, I. (1996). Whose teeth? *Nature* 381, 201-202.

Schwartz, J. H., Long, V. T., Cuong, N. L., Kha, L. T., & Tattersall, I. (1994). A diverse hominoid fauna from the late middle Pleistocene breccia cave of Tham Khuyen, Socialist Republic of Vietnam (excluding Hylobatidae). *Anthropological Papers of the American Museum of Natural History,* 73, 1-11.

Schwartz, J. H., Long, V. T., Cuong, N. L., Kha, L. T., & Tattersall, I. (1995). A review of the Pleistocene hominoid fauna of the Socialist Republic of Vietnam (excluding Hylobatidae). *Anthropological Papers of the American Museum of Natural History,* 76, 1-24.

Selenka, E. (1898). Menschenaffen (Anthropomorphae): Studien Über Entwickelung und Schädelbau; Zur Vergleichenden Keimesgeschichte der Primaten. Wiesbaden, Germany: C. W. Kreidel.

Skinner, M. M., & Gunz, P. (2010). The presence of accessory cusps in chimpanzee lower molars is consistent with a patterning cascade model of development. *Journal of Anatomy,* 217, 245-253.

Skinner, M.M., Wood, B.A., Boesch, C., Olejniczak, A.J., Rosas, A., Smith, T.S., & Hublin, J.-J. (2008). Dental trait expression at the enamel-dentine junction of lower molars in extant and fossil hominoids. *Journal of Human Evolution*, 54, 173-186.

Skinner, M. M., Gunz, P., Wood, B. A., Boesch, C., & Hublin, J.-J. (2009). Discrimination of extant *Pan* species and subspecies using the enamel-dentine junction morphology of lower molars. *American Journal of Physical Anthropology*, 140, 234-243.

Smith, T. M. (2016). Dental development in living and fossil orangutans. *Journal of Human Evolution,* 94, 92-105.

Smith, T. M., Olejniczak, A. J., Reid, D. J., Ferrell, R. J., & Hublin, J.-J. (2006). Modern human molar enamel thickness and enamel-dentine junction shape. *Archives of Oral Biology,* 51, 974-995.

Smith, T. M., Olejniczak, A. J.; Kupczik, K., Lazzari, V., de Vos, J., Kullmer, O., Schrenk, F., Hublin, J.-J., Jacob, T., & Tafforeau. P. (2009). Taxonomic assessment of the Trinil

molars using non-destructive 3D structural and developmental analysis. *PaleoAnthropology*, 117-129.

Smith, T. M., Bacon, A.-M., Demeter, F., Kullmer, O., Nguyen, K. T., de Vos, J., Wei, W., Zermeno, J. P., & Zhao, L. (2011). Dental tissue proportions in fossil orangutans from mainland Asia and Indonesia. *Human Origins Research,* 1, e1ee6.

Smith, T. M., Houssaye, A., Hublin, J.-J., Kato, A., Kullmer, O., Maire, E., Olejniczak, A. J., Schrenk, F., Tafforeau, P., de Vos, J., Zermeno, J. P. (2012). Reassessing enigmatic Asian hominoid dental remains. *American Journal of Physical Anthropology,* S54, 273.

Smith, T. M., Houssaye, A., Kullmer, O., Le Cabec, A., Olejniczak, A. J., Schrenk, F., de Vos, J., Tafforeau, P. (2018). Disentangling isolated dental remains of Asian Pleistocene hominins and pongines. *PLoS ONE,* 13, e0204737.

Spehar, S.N., Sheil, D., Harrison, T., Louys, J., Ancrenaz, M., Marshall, A.J., Wich, S.A., Bruford, M.W., & Meijaard, E. (2018). Orangutans venture out of the rainforest and into the Anthropocene. *Science Advances*, 4, e1701422.

Stevens, N.J., Seiffert, E.R., O'Connor, P.M., Roberts, E.M., Schmitz, M.D., Krause, C., Gorscak, E., Ngasala, S., Hieronymus, T.L., & Temu, J. (2013). Palaeontological evidence for an Oligocene divergence between Old World monkeys and apes. *Nature,* 497, 611-614.

Suwa, G., Kono, R., Katoh, S., Asfaw, B., & Beyene, Y. (2007). A new species of great ape from the late Miocene epoch in Ethiopia. *Nature,* 448, 921-924.

Swindler, D. R. (1976) *Dentition of living primates*. London, UK: Academic Press.

Swindler, D. R, & Olshan, A. F. (1988). Comparative and evolutionary aspects of permanent dentition. In J. H. Schwartz (Ed.), *Orang-utan Biology* (pp 271-282). New York, NY: Oxford University Press.

Szalay, F. S. (1969). Mixodectidae, Microsyopidae, and the insectivore-primate transition. *Bulletin of the American Museum of Natural History,* 140, 193-330.

Szalay, F., & Delson, E. (1979) *Evolutionary history of the primates*. New York, NY: Academic Press.

Swisher, C.C. 3rd, Curtis, G. H., Jacob, T., Getty, A. G., Suprijo, A., & Widiasmoro, (1994). Age of the earliest known hominids in Java, Indonesia. *Science,* 263, 1118-1121.

Tshen, L. T. (2016). Biogeographic distribution and metric dental variation of fossil and living orangutans (*Pongo* spp.). *Primates,* 57, 39-50.

Tuniz, C., Bernardini, F., Cicuttin, A., Crespo, M.L., Dreossi, D., Gianoncelli, A., Mancini, L., Mendoza Cuevas, A., Sodini, N., Tromba, G., Zanini, F., Zanolli, C. (2013). The ICTP-Elettra X-ray laboratory for cultural heritage and archaeology. A facility for training and education in the developing world. *Nuclear Instruments and Methods*, A 711, 106-110.

Turner, C. G., Nichol, C. R., & Scott, G. R. (1991). Scoring procedures for key morphological traits of the permanent dentition: the Arizona State University Dental Anthropology System. In M. A. Kelley, C. S. Larsen (Eds.), *Advances in Dental Anthropology* (pp. 13-31). New York, NY: Wiley-Liss.

Tyler, D. E. (1991). A taxonomy of Javan hominid mandibles. *Human Evolution*, 6, 401-420.

Tyler, D. E. (1995). The current picture of hominid evolution in Java. *Acta Anthropologica Sinica*, 14, 313-323.

Tyler, D. E. (2004). An examination of the taxonomic status of the fragmentary mandible Sangiran 5, (*Pithecanthropus dubius*), *Homo erectus*, ‘‘*Meganthropus*’’, or *Pongo*? *Quaternary International,* 117, 125-130.

Uchida, A. (1996). *Craniodental variation among the great apes*. Cambridge, MA: Peabody Museum of Archaeology and Ethnology, Harvard University.

Uchida, A. (1998). Variation in tooth morphology of *Pongo pygmaeus*. *Journal of Human Evolution,* 34, 71-79.

Van Valen, L. (1966). Deltatheridia, a new order of mammals. *Bulletin of the American Museum of Natural History,* 132, 1-126.

von Koenigswald, G.H.R. (1952). *Gigantopithecus blacki* von Koenigswald, a giant fossil hominoid from the Pleistocene of Southern China. *Anthropological Papers of the American Museum of Natural History,* 43, 295-325.

von Koenigswald, G. H. R. (1982). Distribution and evolution of the orang utan, *Pongo pygmaeus* (Hoppius). In L. E. M. de Boer (Ed.), *The Orang utan. Its Biology and Conservation* (pp. 1-15), The Hague, Netherlands: W. Junk Publishers.

Wang, C. B., Zhao, L. X., Jin, C. Z., Wang, Y., Qin, D. G., & Pan, W. S. (2014). New discovery of Early Pleistocene orangutan fossils from Sanhe Cave in Chongzuo, Guangxi, southern China. *Quaternary International,* 354, 68-74.

Weidenreich, F. (1945). Giant early man from Java and South China. *Anthropological Papers of the American Museum of Natural History,* 40: 1-134.

Weidenreich, F. (1973). The dentition of *Sinanthropus pekinensis*: A comparative odontography of the hominids. *Palaeontologia Sinica,* 1, 120-180.

Wollny, G., Kellman, P., Ledesma-Carbayo, M.-J., Skinner, M. M., Hublin, J.-J., & Hierl, T. (2013). MIA – a free and open source software for gray scale medical image analysis. *Source Code for Biology and Medicine,* 8, 20.

Zanolli, C., Bondioli, L., Coppa, A., Dean, M.C., Bayle, P., Candilio, F., Capuani, S., Dreossi, D., Fiore, I., Frayer, D.W., Libsekal, Y., Mancini, L., Rook, L., Medin, T., Tuniz, C., & Macchiarelli, R. (2014). The late Early Pleistocene human dental remains from Uadi Aalad and Mulhuli-Amo (Buia), Eritrean Danakil: Macromorphology and microstructure. *Journal of Human Evolution*, 74, 96-113.

Zanolli, C., Grine, F. E., Kullmer, O., Schrenk, F., & Macchiarelli, R. (2015). The Early Pleistocene deciduous hominid molar FS-72 from the Sangiran Dome of Java, Indonesia: A taxonomic reappraisal based on its comparative endostructural characterization. *American Journal of Physical Anthropology,* 157, 666-674.

Zanolli, C., Kullmer, O., Kelley, J., Bacon, A.-M., Demeter, F., Dumoncel, J., Fiorenza, L., Grine, F.E., Hublin, J.-J., Nguyen Anh Tuan, Nguyen Thi Mai Huong, Pan, L., Schillinger, B., Schrenk, F., Skinner, M.M., Ji, X., & Macchiarelli, R. (2019). Evidence for increased hominid diversity in the Early-Middle Pleistocene of Java, Indonesia. *Nature Ecology and Evolution* (in press).

Zanolli, C., Pan, L., Dumoncel, J., Kullmer, O., Kundrát, M., Liu, W., Macchiarelli, R., Mancini, L., Schrenk, F., & Tuniz, C. (2018). Inner tooth morphology of *Homo erectus* from Zhoukoudian. New evidence from an old collection housed at Uppsala University, Sweden. *Journal of Human Evolution*, 116, 1-13.

Zhang, Z., & Harrison, T. (2008). A new middle Miocene pliopithecid from Inner Mongolia, China. *Journal of Human Evolution,* 54, 444-447.

Zhang, Y. & Harrison, T. (2017). *Gigantopithecus blacki*: a giant ape from the Pleistocene of Asia revisited. *American Journal of Physical Anthropology,* 162, 153-177.

Zhang, Y.-Q., Jin, C.-Z., Wang, Y., Ortiz, A., He, K., & Harrison, T. (2018). Fossil gibbons (Mammalia, Hylobatidae) from the Pleistocene of Chongzuo, Guangxi, China. *Vertebrata PalAsiatica,* 56, 248-263.

Zhao, L. X., Wang, C. B., Jin, C. Z., Qin, D. G., & Pan, W. S. (2009). Fossil orangutan-like hominoid teeth from Late Pleistocene human site of Mulanshan Cave in Chongzuo of Guangxi and implications on taxonomy and evolution of orangutan. *Chinese Science Bulletin*, 54, 3924-3930.

Zhu, R. X., Potts, R., Pan, Y. X., Yao, H. T., Lu, L. Q., Zhao, X., Gao, X., Chen, L. W., Gao, F., & Deng, C. L. (2008). Early evidence of the genus *Homo* in East Asia. *Journal of Human Evolution,* 55, 1075-1085.

Zhu, Z. Y., Dennell, R., Huang, W. W., Wu, Y., Rao, Z. G., Qiu, S. F., Xie, J. B., Liu, W., Fu, S. Q., Han, J. W., Zhou, H. Y., Yang, T. P. O., & Li, H. M. (2015). New dating of the *Homo erectus* cranium from Lantian (Gongwangling), China. *Journal of Human Evolution,* 78, 144-157.

Zhu, Z. Y., Dennell, R., Huang, W. W., Wu, Y., Qiu, S. F., Yang, S., Rao, Z. G., Hou, Y., Xie, J. B., Han, & Ouyang, T.P. (2018). Hominin occupation of the Chinese Loess Plateau since about 2.1 million years ago. *Nature*, 559, 608-612.

**Figure Legends**

**Fig. 1.** Scoring system of protoconule expression at the EDJ of hominoid molars. (a) Grade 0: protoconule is absent; (b) Grade 1A ("suspected" category): faint furrows, bumps, and other barely discernible irregularities are present; (c) Grade 1B ("suspected" category): a weak pointed elevation is present that may represent a poorly developed dentine horn; (d) Grade 2: a moderate protoconule is present; and (e) Grade 3: a large protoconule is present. Mesial views. Left molars depicted. Lingual aspect to the right.

**Fig. 2.** Landmarks and semi-landmarks used in the mesial fovea shape analysis. Big and small yellow circles correspond to landmarks and semi-landmarks, respectively. Landmark/semi-landmark order in red font.

**Fig. 3.** Frequencies of protoconule expression in hominid upper molars. (a) Comparisons at the generic level, all molars combined; (b) Comparisons between members of *Homo* and *Pongo* at the species level, all molars combined; and (c) Comparisons between *Homo* and *Pongo* at the generic level, first (M1), second (M2) and third (M3) molars analyzed independently. AUS:

*Australopithecus*; PAR: *Paranthropus*; HOMO: *Homo*; PAN: *Pan*; GOR: *Gorilla*; PONGO: *Pongo*; MEGA: *Meganthropus*; SIVA: *Sivapithecus*; EHOM: early *Homo*; HERE: *H. erectus*; HN: *H. neanderthalensis*; HSP: Pleistocene *H. sapiens*; HSR: recent *H. sapiens*; PONEXT: extant *Pongo*; PONCH: Pleistocene *Pongo* from China; and PONVI: Pleistocene *Pongo* from Vietnam. Orange: grade 0; gray: grade 1A; green: grade 1B; purple: grade 2; and red: grade 3.

**Fig. 4.** Upper molars of Pleistocene *Pongo* from China with different degrees of protoconule expression. (a-c) Grade 1A; (d-f) grade 2; and (g-i) grade 3. Mesial views. Left molars depicted (right specimens mirror-imaged where applicable). Lingual aspect to the right. Specimens depicted: a. DLZNH 201211-15 M1; b. DLZNH 201211-23 M2; c. DLZNH 201211-524 M3; d. DLZNH 201206-5 M3; e. DLZNH 201211-21 M3; f. DLZNH 201211-22 M3; g. DLZNH 201206-12 M1; h. DLZNH 201211-534 M1; i. DLZNH 201211-538 M3.

**Fig. 5.** Upper molars of Pleistocene *Pongo* from Vietnam with different degrees of protoconule expression. (a-c) Grade 1A; (d-f) grade 2; and (g-i) grade 3. Mesial views. Left molars depicted (right specimens mirror-imaged where applicable). Lingual aspect to the right. Specimens depicted: a. 93LT4; b. 93LT40; c. HH53; d. 77.TO.o.10.A.20; e. 77.TO.o.13.21; f. HH38; g. 77.TO.13.XX; h. 93LT7; i. 93LT38.

**Fig. 6.** Upper molars of extant *Pongo* with different degrees of protoconule expression. (a-b) grade 1A; (c) grade 1B, (d-f) grade 2; and (g-i) grade 3. Mesial views. Left molars depicted. Lingual aspect to the right.

**Fig. 7.** Upper molars of *H. erectus s.l.* with different degrees of protoconule expression. (a) grade 0; (b-c) grade 1A; (d) grade 1B (note a larger accessory tubercle on the mesial marginal ridge; see arrow). Mesial views. Left molars depicted (right specimens mirror-imaged where applicable). Lingual aspect to the right. Specimens depicted: a. KNM-ER 1808H M2; b. S4 M1; c. S7-3b M1; d. S4 M3.

**Fig. 8.** Upper molars of *H. sapiens* with different degrees of protoconule expression. (a) grade 0; (b-c) grade 1A; (d) grade 1B; (e-f) grade2. Mesial views. Left molars depicted. Lingual aspect to the right.

**Fig. 9.** Upper molars of *Sivapithecus* (a-c) and *Meganthropus* (d-e) with different degrees of protoconule expression. (a-c) grade 2; (d) grade 0 (note a large accessory tubercle on the mesial marginal ridge; see arrow); (e) grade 1A (note a medium-sized accessory tubercle on the mesial marginal ridge; see arrow). Mesial views. Left molars depicted (right specimens mirror-imaged where applicable). Lingual aspect to the right. Specimens depicted: a. GSP 17919; b. GSP 31101; c. GSP 47586; d. Trinil 11620; Trinil 11621.

Fig. 10. Plot of the first two discriminant functions of mesial fovea shape in M1-M3 combined. All species of fossil and extant hominids included. See also Table 2. Symbols: *Australopithecus* (squares), *Paranthropus* (squares), early *Homo* (dots), *H. erectus* (stars), *H. neanderthalensis* (dots), *H. sapiens* (dots), *Pan* (triangles), *Gorilla* (inverted triangles), *Meganthropus* (stars), *Sivapithecus* (open diamonds), extant *Pongo* (diamonds), fossil *Pongo* China (diamonds), and fossil *Pongo* Vietnam (diamonds).

**Fig. 11.** Plot of the first two discriminant functions of mesial fovea shape in M1-M3 combined. Only species from *Homo* and *Pongo* included. See also Table S8. Symbols: early *Homo* (dots), *H. erectus* (stars), *H. neanderthalensis* (dots), *H. sapiens* (dots), extant *Pongo* (diamonds), fossil *Pongo* China (diamonds), and fossil *Pongo* Vietnam (diamonds).

**Fig. 12.** Comparisons of mesial fovea variation between (A) extant and fossil *Pongo*, (B) *H. erectus* and fossil *Pongo*, and (C) *Homo* and *Pongo* based on mean shapes at the EDJ of M1-M3 combined. Wireframes depict left molars. Mahalanobis distances for (A) 5.583, (B) 7.768, and (C) 11.136. All distances significant at $p < 0.01$.

**Table 1.** Upper molars of fossil and extant hominids used in this study.

| Taxon | UM1 | UM2 | UM3 | UM | Total |
|---|---|---|---|---|---|
| *A. anamensis* | 1 | 2 | - | - | 3 |
| *A. afarensis* | 3 | 1 | 2 | 1 | 7 |
| *A. africanus* | 10 | 14 | 15 | - | 39 |
| *P. robustus* | 13 | 14 | 14 | - | 41 |
| *P. boisei* | 1 | 1 | 2 | - | 4 |
| early *Homo* | 4 | 3 | 1 | - | 8 |
| *H. erectus s.l.* | 2 | 3 | 1 | 1 | 7 |
| MPEH | 1 | 1 | 1 | - | 3 |
| *H. neanderthalensis* | 19 | 22 | 15 | 1 | 57 |
| Pleistocene *H. sapiens* | 5 | 7 | 3 | 3 | 18 |
| recent *H. sapiens* | 18 | 35 | 11 | 13 | 77 |
| *P. troglodytes* | 16 | 27 | 15 | - | 58 |
| *P. paniscus* | 6 | 3 | - | - | 9 |
| *Gorilla* sp. | 5 | 12 | 11 | - | 28 |
| *Meganthropus* sp. | - | - | - | 2 | 2 |
| *Sivapithecus* sp. | - | - | - | 3 | 3 |
| recent *Pongo* | | | | | |
| *P. abelii* | 5 | 4 | 3 | - | 12 |
| *P. pygmaeus* | 2 | 3 | 3 | - | 8 |
| *Pongo* sp. | 4 | 3 | 3 | - | 10 |
| Pleistocene *Pongo* (China) | 10 | 5 | 10 | - | 25 |
| Pleistocene *Pongo* (Vietnam) | 1 | 0 | 7 | 42 | 50 |

MPEH: Middle Pleistocene European hominins

**Table 2.** Discriminant model accuracy results for mesial fovea shape variation and percent of the variation accounted for by each axis. All species of fossil and extant hominids included.

| CVA Hominoidea | M1-M3* | M1-M3** | M1 | M2 | M3 |
|---|---|---|---|---|---|
| Total | 364 | 359 | 122 | 132 | 101 |
| Model accuracy (without resampling) | 71.68% | 84.96% | 94.60% | 93.18% | 91.09% |
| Model accuracy (with resampling) | 60.85% | 71.36% | 68.03% | 66.67% | 52.48% |
| Axis 1 - % Variation | 41.17 | 33.13 | 36.54 | 36.98 | 38.41 |
| Axis 1 - Eigenvalue | 3.041 | 3.065 | 4.786 | 5.315 | 4.51 |
| Axis 2 - % Variation | 26.94 | 23.49 | 20.84 | 23.88 | 18.25 |
| Axis 2 - Eigenvalue | 1.990 | 2.173 | 2.73 | 3.433 | 2.142 |
| Axis 3 - % Variation | 11.17 | 14.32 | 13.01 | 14.85 | 13.85 |
| Axis 3 - Eigenvalue | 0.825 | 1.325 | 1.704 | 2.135 | 1.627 |
| Axis 4 - % Variation | 7.83 | 10.66 | 8.85 | 7.829 | 12.76 |
| Axis 4 - Eigenvalue | 0.578 | 0.986 | 1.159 | 1.124 | 1.499 |

* Genera included: *Australopithecus*, *Paranthropus*, *Homo*, *Meganthropus*, *Sivapithecus*, *Pan*, *Gorilla*, and *Pongo*;
** Genera included: *Australopithecus*, *Paranthropus*, *Homo*, *Pan*, *Gorilla*, and *Pongo*

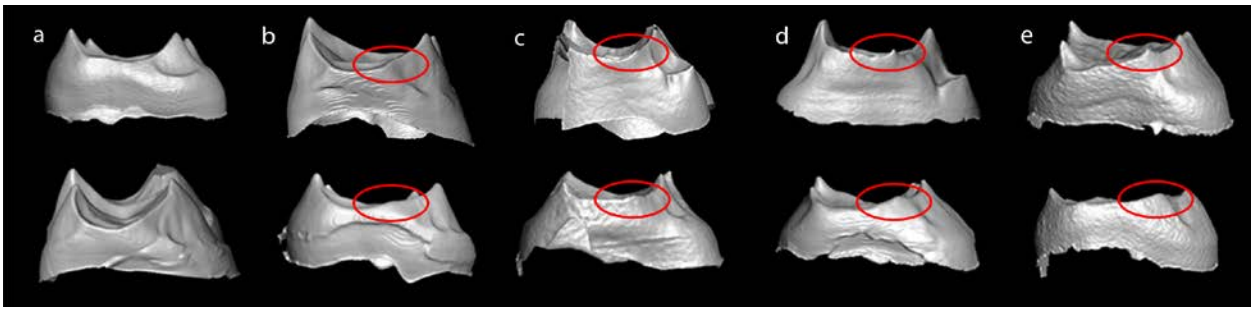

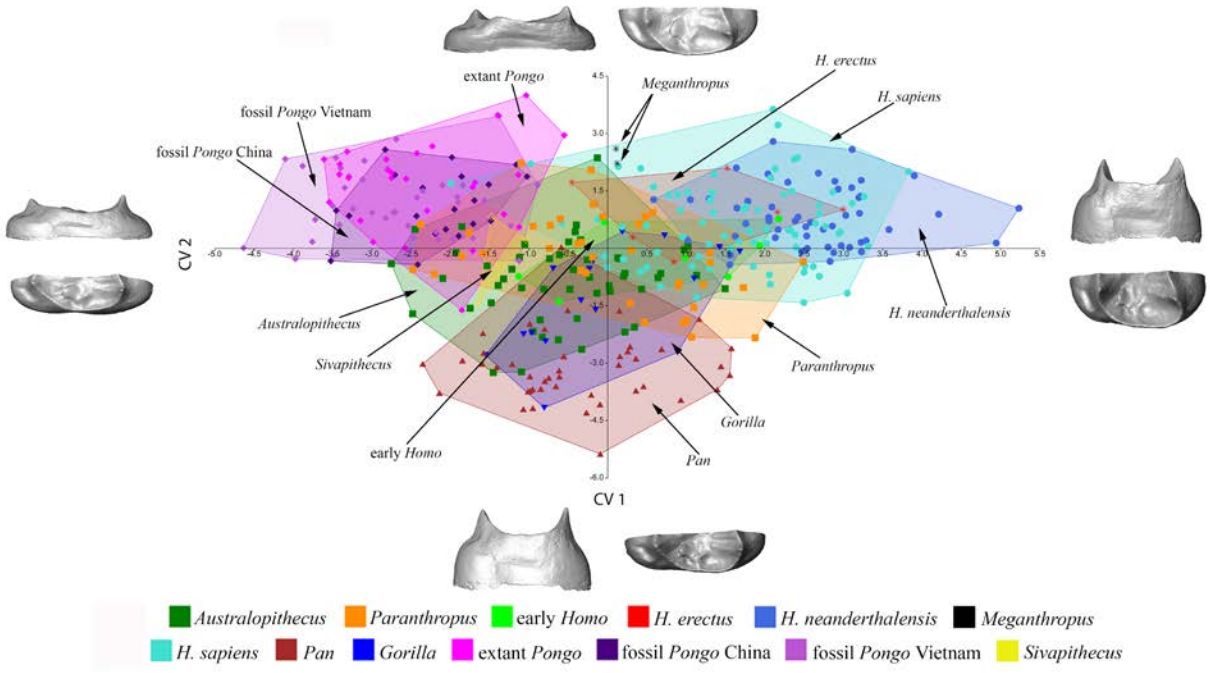

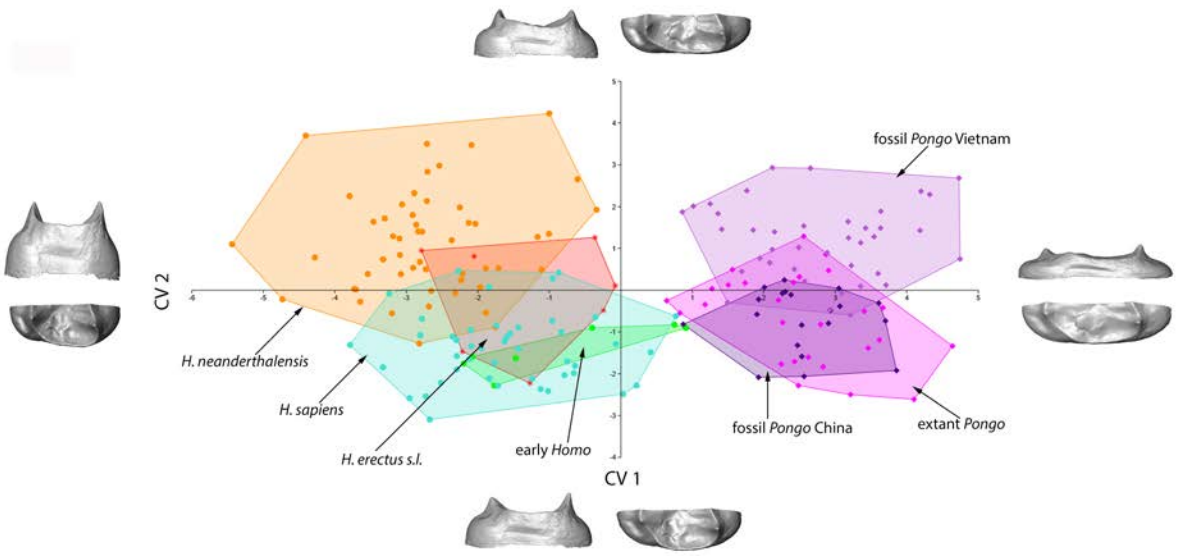

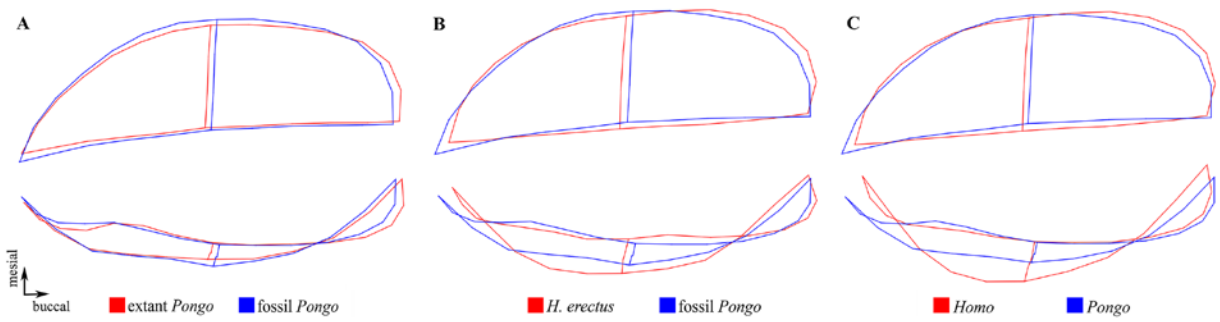

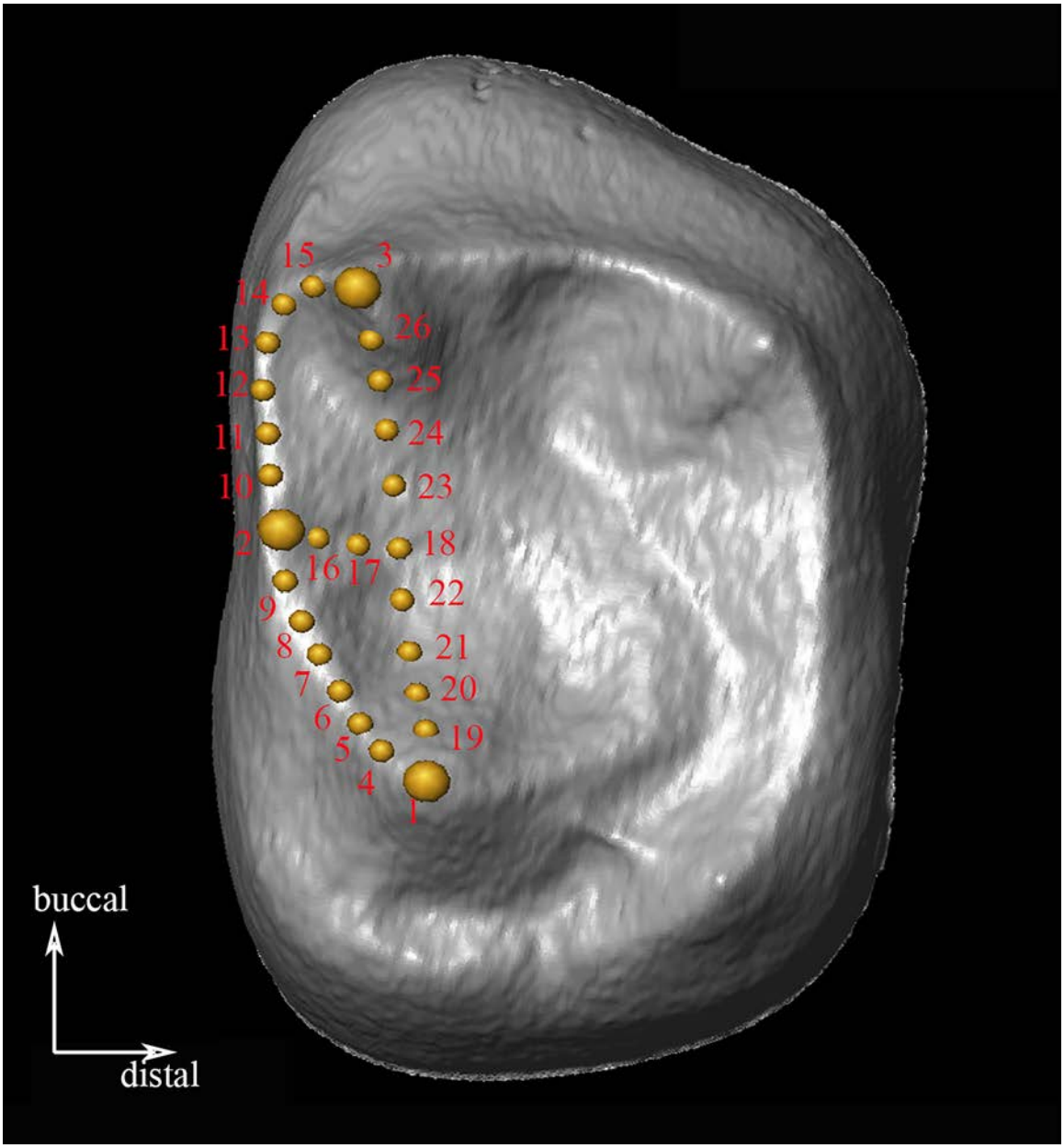

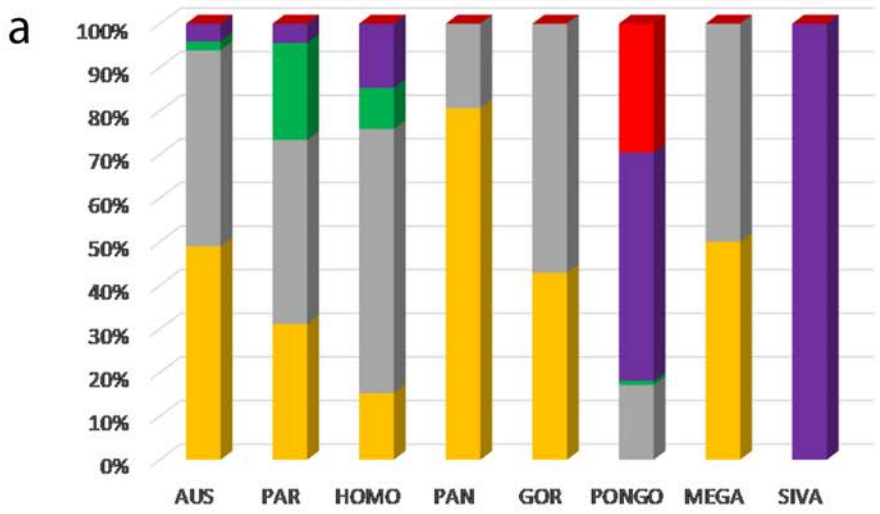


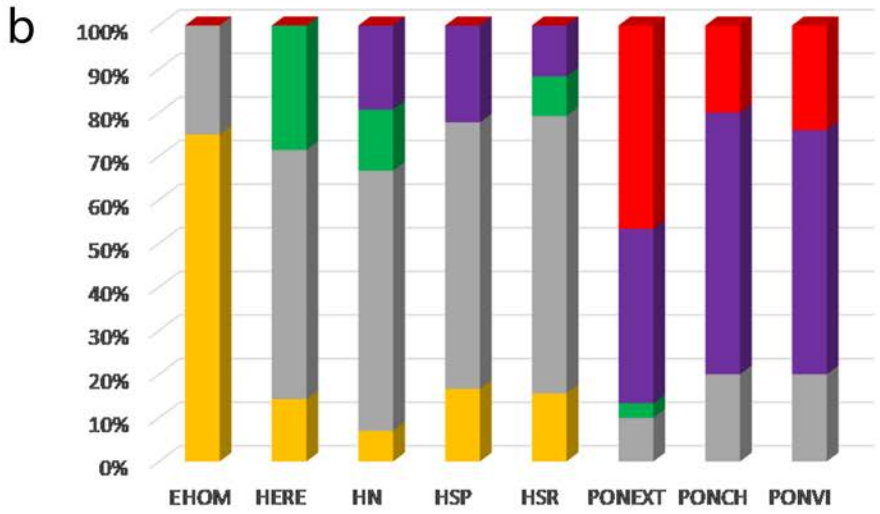


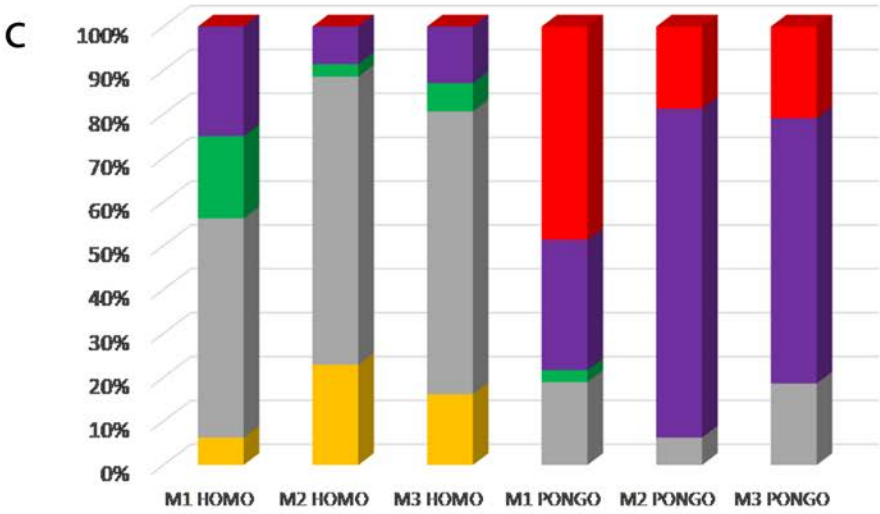

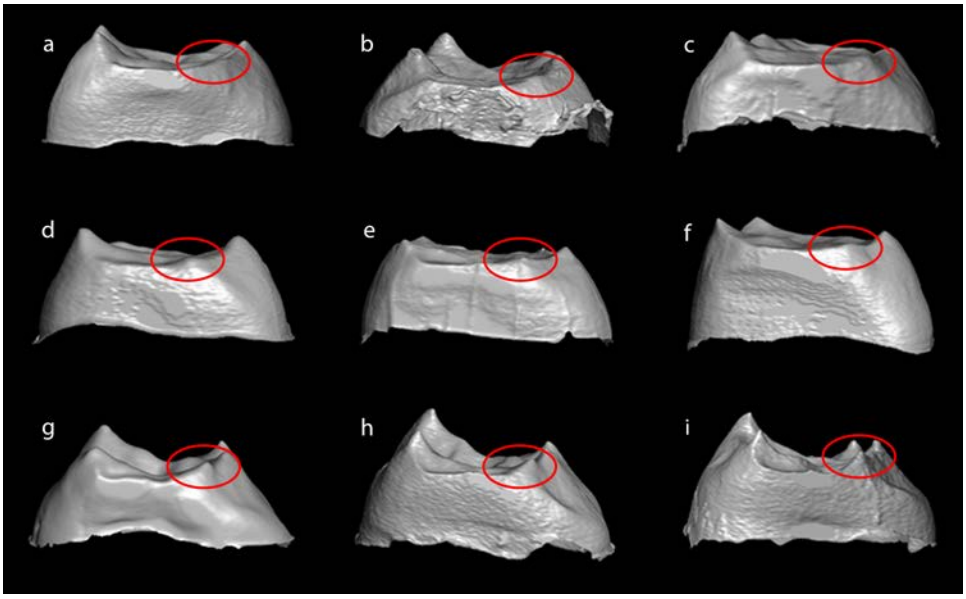

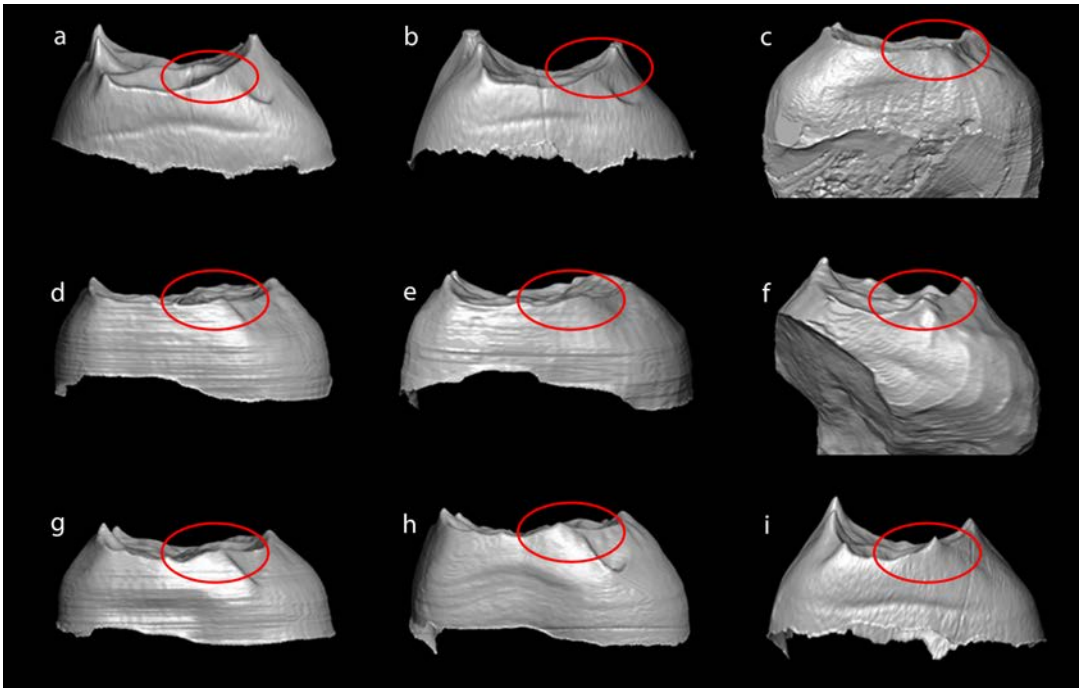

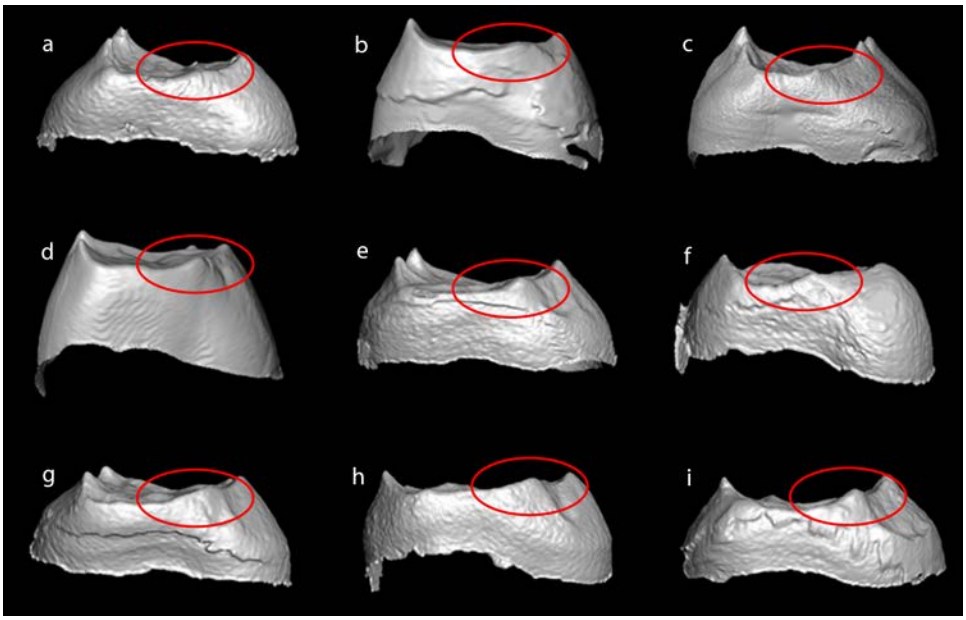

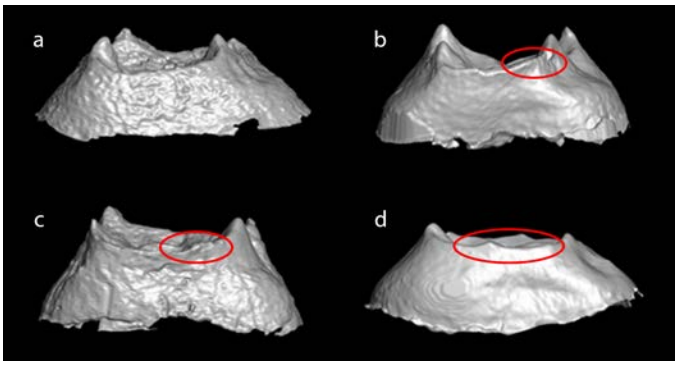

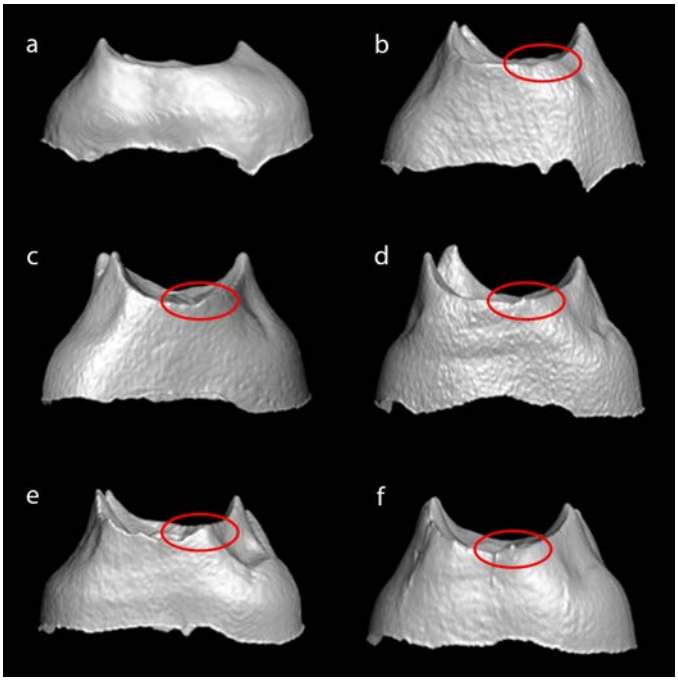

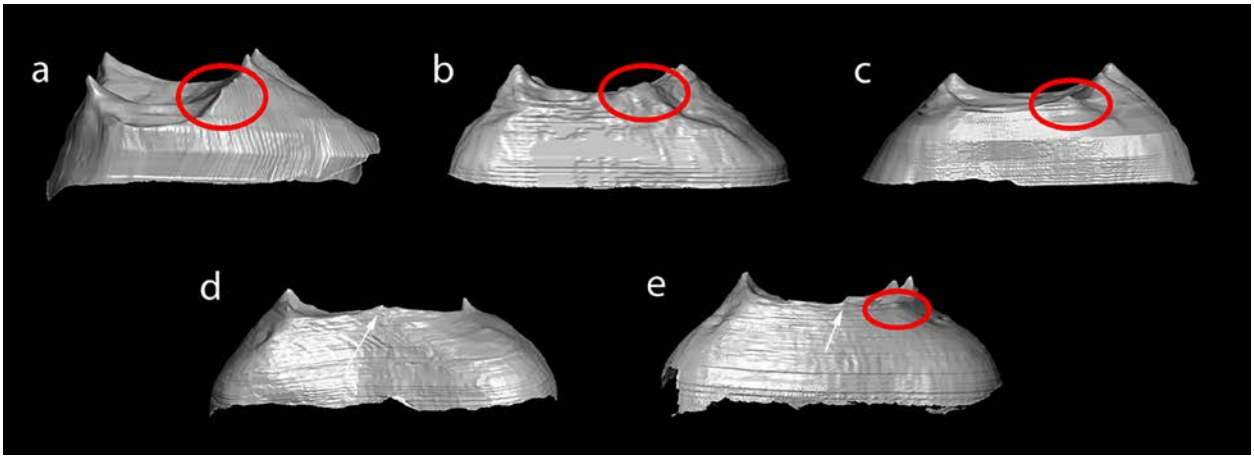

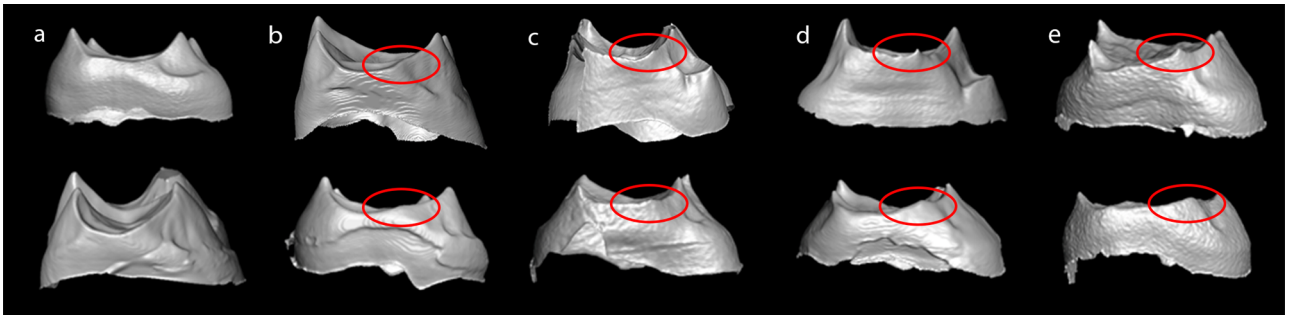


AJPA_23928_Fig. 1.tif

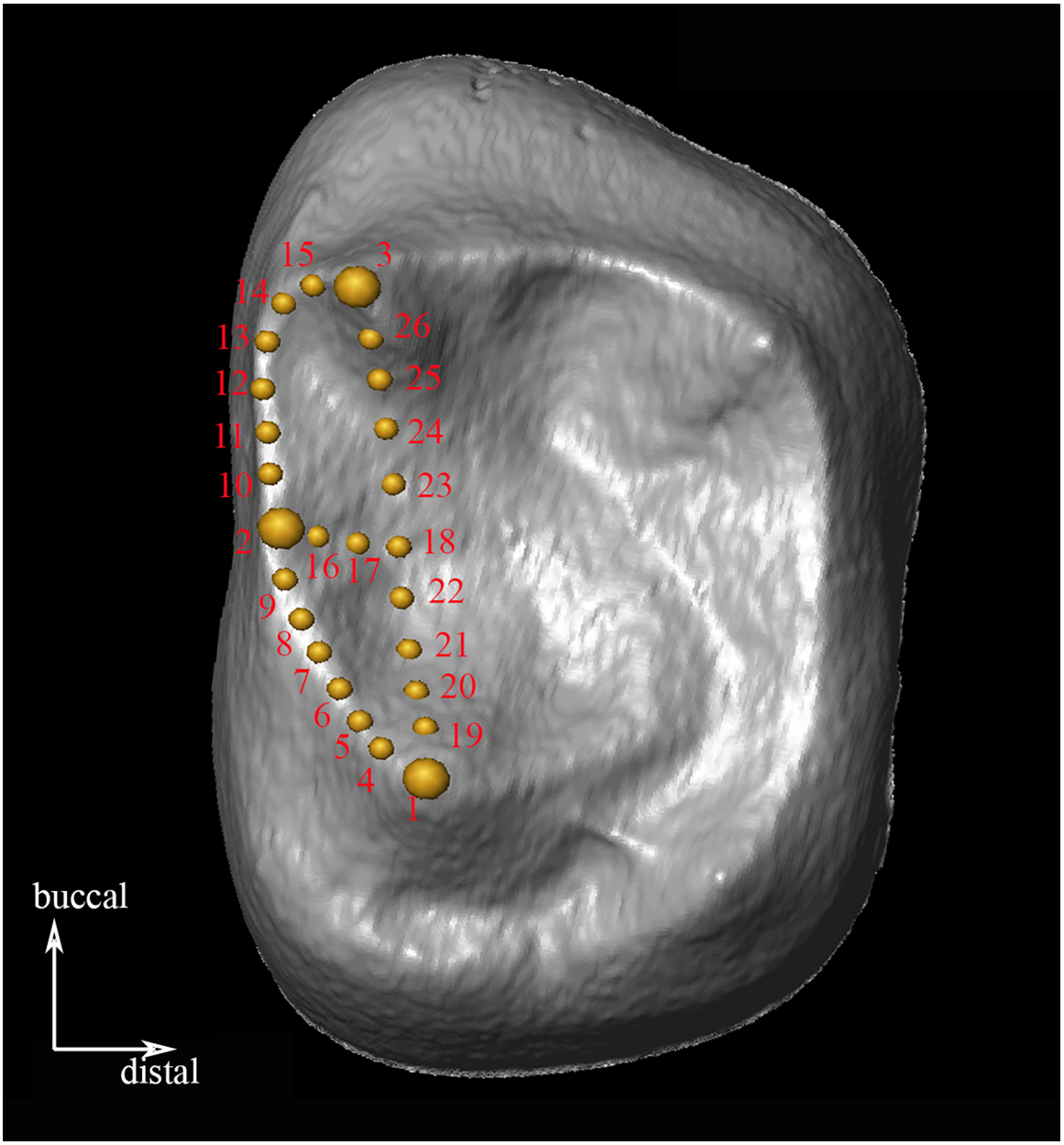


AJPA_23928_Fig. 2.tif

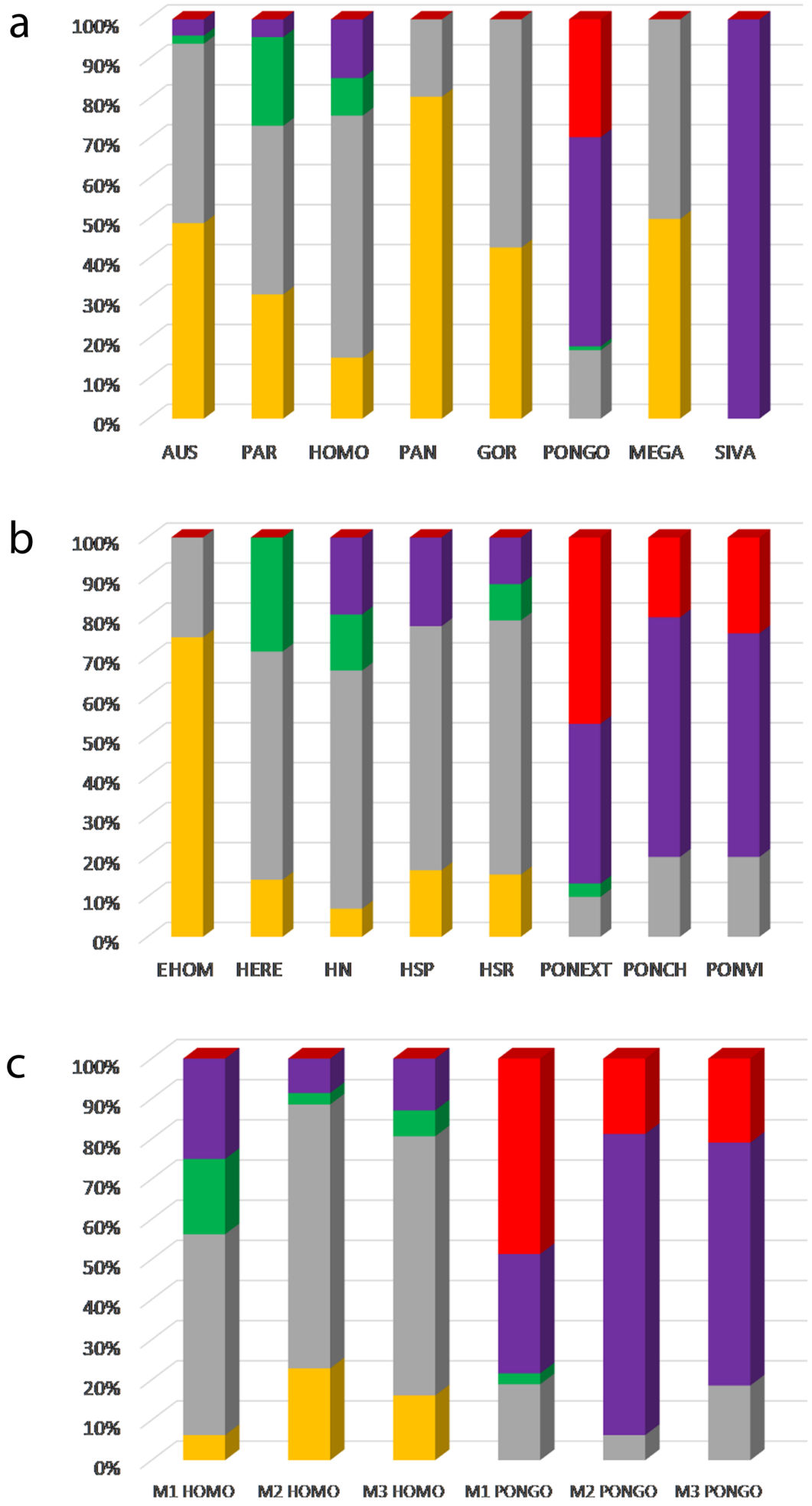


AJPA_23928_Fig. 3_rev.tif

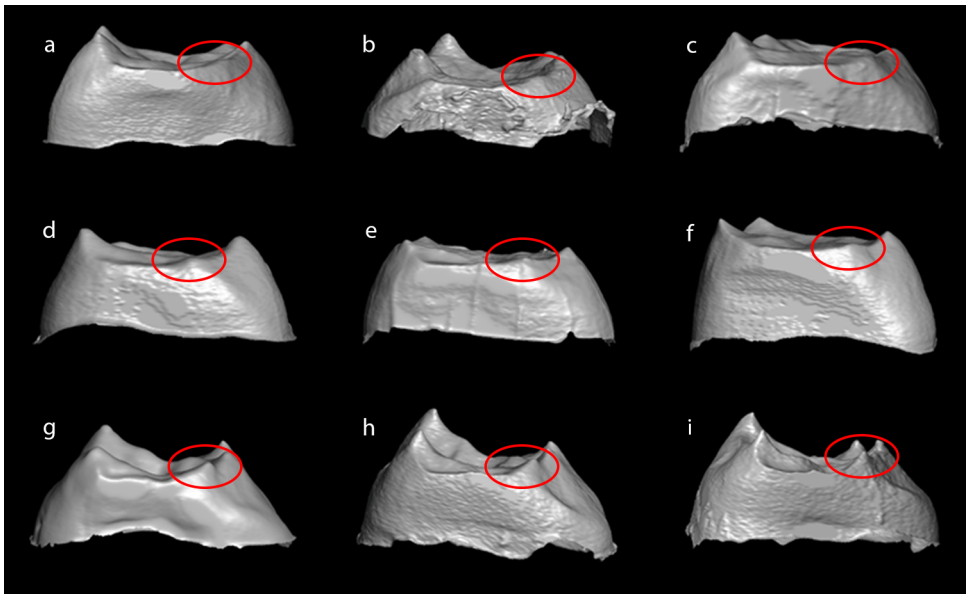


AJPA_23928_Fig. 4.tif

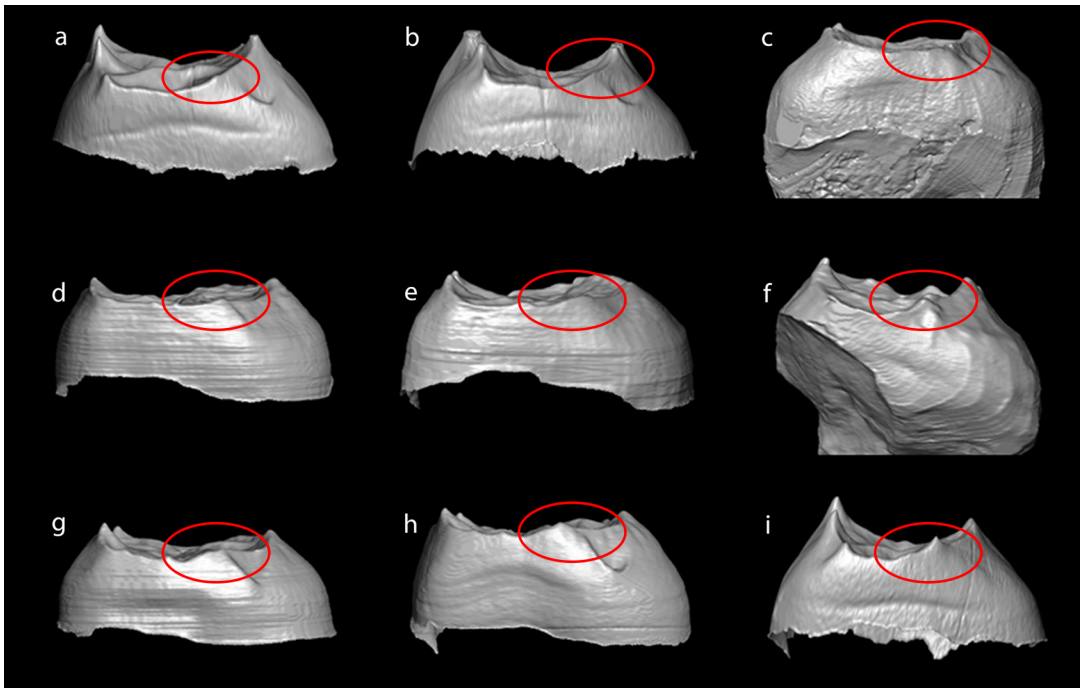


AJPA_23928_Fig. 5.tif

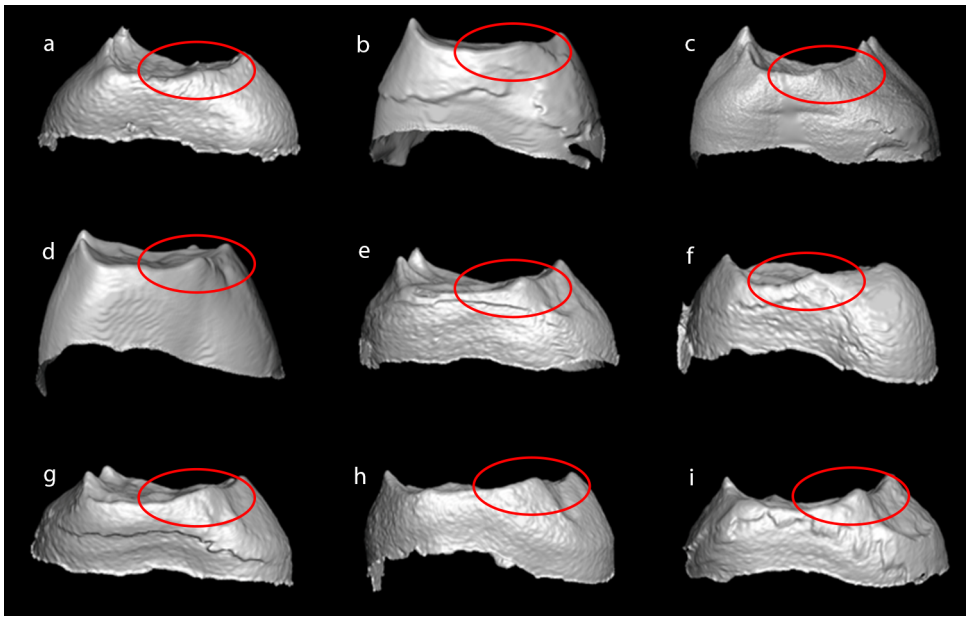


AJPA_23928_Fig. 6.tif

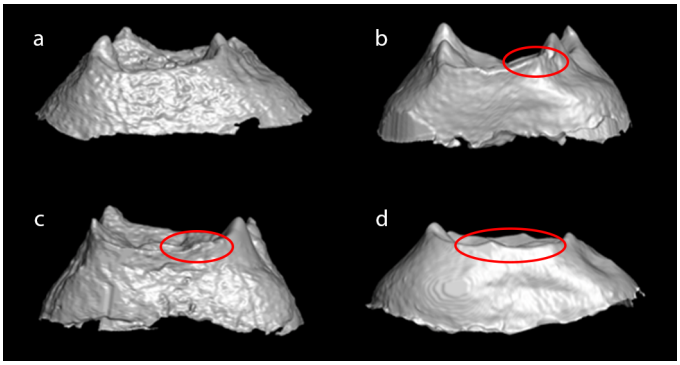


AJPA_23928_Fig. 7.tif

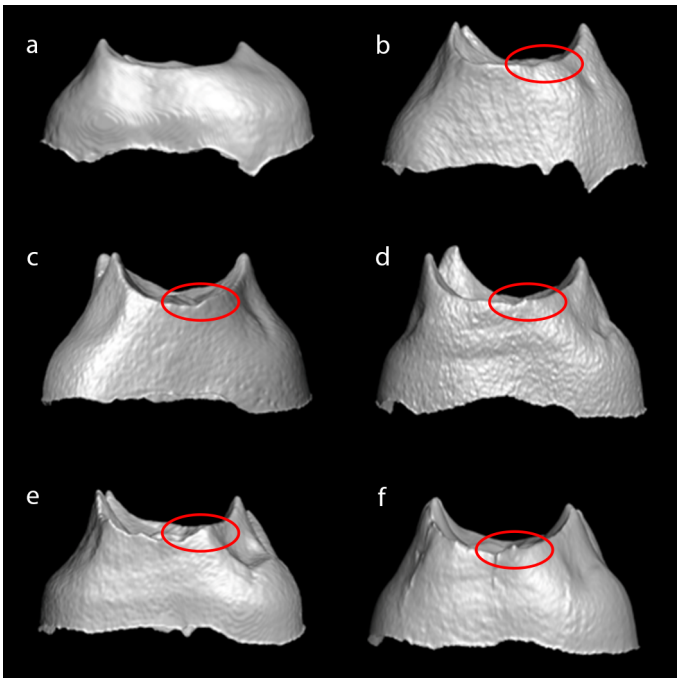


AJPA_23928_Fig. 8.tif

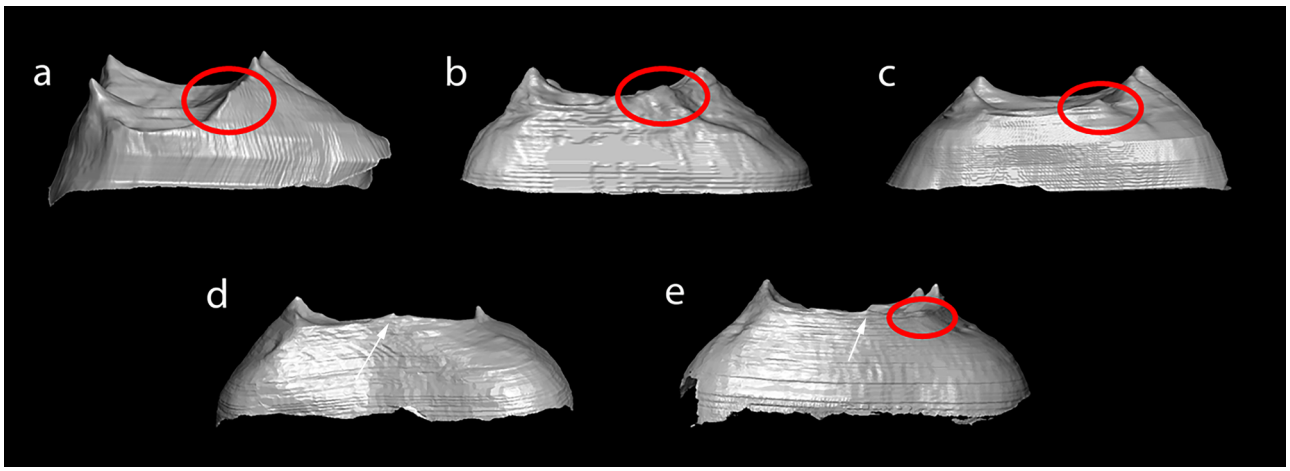


AJPA_23928_Fig. 9_rev.tif

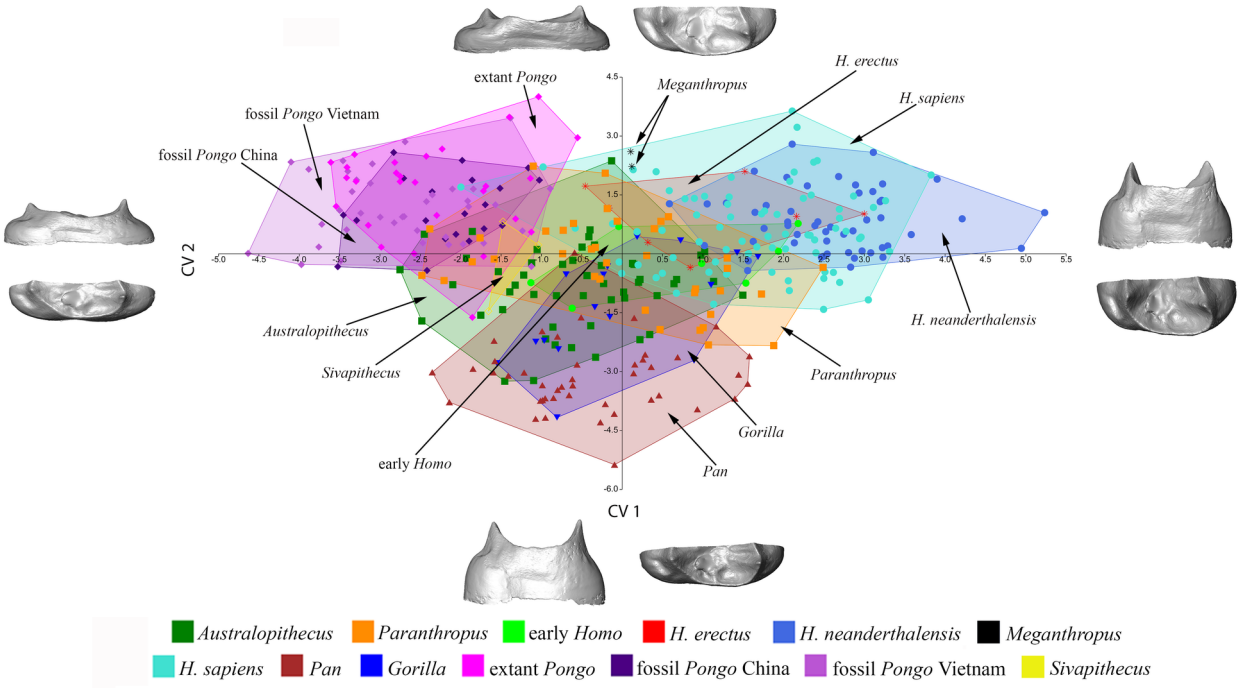


AJPA_23928_Fig. 10_rev.tif

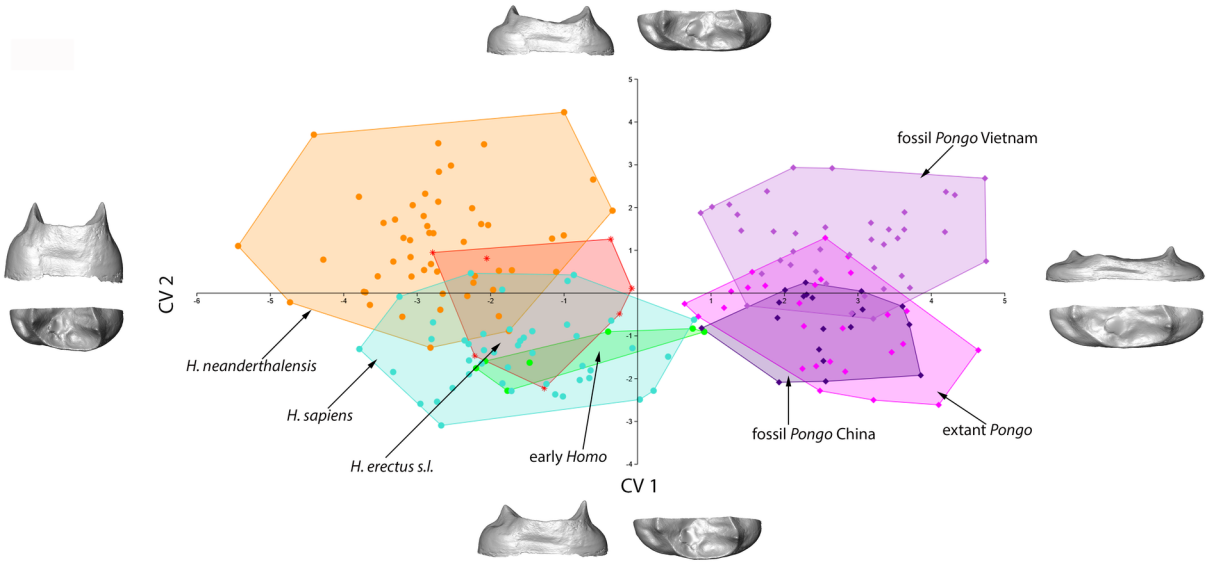


AJPA_23928_Fig. 11_rev.tif

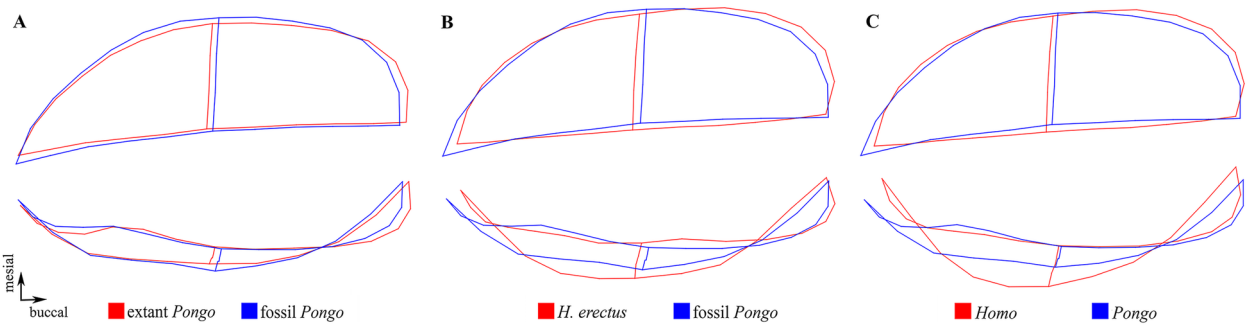


AJPA_23928_Fig. 12.tif

**Table 1.** Upper molars of fossil and extant hominids used in this study.

| Taxon | UM1 | UM2 | UM3 | UM | Total |
|---|---|---|---|---|---|
| *A. anamensis* | 1 | 2 | - | - | 3 |
| *A. afarensis* | 3 | 1 | 2 | 1 | 7 |
| *A. africanus* | 10 | 14 | 15 | - | 39 |
| *P. robustus* | 13 | 14 | 14 | - | 41 |
| *P. boisei* | 1 | 1 | 2 | - | 4 |
| early *Homo* | 4 | 3 | 1 | - | 8 |
| *H. erectus s.l.* | 2 | 3 | 1 | 1 | 7 |
| MPEH | 1 | 1 | 1 | - | 3 |
| *H. neanderthalensis* | 19 | 22 | 15 | 1 | 57 |
| Pleistocene *H. sapiens* | 5 | 7 | 3 | 3 | 18 |
| recent *H. sapiens* | 18 | 35 | 11 | 13 | 77 |
| *P. troglodytes* | 16 | 27 | 15 | - | 58 |
| *P. paniscus* | 6 | 3 | - | - | 9 |
| *Gorilla* sp. | 5 | 12 | 11 | - | 28 |
| *Meganthropus* sp. | - | - | - | 2 | 2 |
| *Sivapithecus* sp. | - | - | - | 3 | 3 |
| recent *Pongo* | | | | | |
| *P. abelii* | 5 | 4 | 3 | - | 12 |
| *P. pygmaeus* | 2 | 3 | 3 | - | 8 |
| *Pongo* sp. | 4 | 3 | 3 | - | 10 |
| Pleistocene *Pongo* (China) | 10 | 5 | 10 | - | 25 |
| Pleistocene *Pongo* (Vietnam) | 1 | 0 | 7 | 42 | 50 |

MPEH: Middle Pleistocene European hominins

**Table 2.** Discriminant model accuracy results for mesial fovea shape variation and percent of the variation accounted for by each axis. All species of fossil and extant hominids included.

| CVA Hominoidea | M1-M3* | M1-M3** | M1 | M2 | M3 |
|---|---|---|---|---|---|
| Total | 364 | 359 | 122 | 132 | 101 |
| Model accuracy (without resampling) | 71.68% | 84.96% | 94.60% | 93.18% | 91.09% |
| Model accuracy (with resampling) | 60.85% | 71.36% | 68.03% | 66.67% | 52.48% |
| Axis 1 - % Variation | 41.17 | 33.13 | 36.54 | 36.98 | 38.41 |
| Axis 1 - Eigenvalue | 3.041 | 3.065 | 4.786 | 5.315 | 4.51 |
| Axis 2 - % Variation | 26.94 | 23.49 | 20.84 | 23.88 | 18.25 |
| Axis 2 - Eigenvalue | 1.990 | 2.173 | 2.73 | 3.433 | 2.142 |
| Axis 3 - % Variation | 11.17 | 14.32 | 13.01 | 14.85 | 13.85 |
| Axis 3 - Eigenvalue | 0.825 | 1.325 | 1.704 | 2.135 | 1.627 |
| Axis 4 - % Variation | 7.83 | 10.66 | 8.85 | 7.829 | 12.76 |
| Axis 4 - Eigenvalue | 0.578 | 0.986 | 1.159 | 1.124 | 1.499 |

* Genera included: *Australopithecus*, *Paranthropus*, *Homo*, *Meganthropus*, *Sivapithecus*, *Pan*, *Gorilla*, and *Pongo*;
** Genera included: *Australopithecus*, *Paranthropus*, *Homo*, *Pan*, *Gorilla*, and *Pongo*